Supporting Information

Bi-component Sensing Platform for Detection of Cd^{2+}, Fe^{2+} and Fe^{3+} ions

Jagajiban Sendh, and Jubaraj B. Baruah

List of Captions

Figure S8 UV-visible titration of (a) Naphydrazide (3 mL) and 2,6-H_2pdc (0.8 mL) (taken together from respective 3.32 μM stock solution in DMF) with each aliquot addition of Zn^{2+} ions followed by addition of (a) Fe^{3+} ions and (b) Fe^{3+} ions (c) Plots of increase in the absorbance at 270 nm of a solution of the above solutions. (d) UV-visible titration of Naphydrazide (3 mL) and 2,6-H_2pdc (0.8 mL) (taken together from respective 3.32 μM stock solution in DMF) with different aliquots of solution of Cd^{2+} ions followed by (d) Fe^{3+} ions and (e) Fe^{2+} ions; (e) The plots of absorbances at 270 nm against concentration of ions from the figures (d) and (e).

Figure S9 Fluorescence excitation (i) and emission spectra (ii) of (a) Naphydrazide (λ_{ex} = 335 nm, λ_{em} = 396 nm) (b) Binaphydrazide (λ_{ex} = 378 nm, λ_{em} = 558 nm) in DMF (3mL of 2mM solution of receptor in each case).

Figure S10 Fluorescence emission titration by adding100 μL, 20 mM Cd^{2+} solution followed by addition of aliquots of 100 μL, 20 mM Cd^{2+} solution to (i) Naphydrazide (2mM, 2500 μL DMF) and 2,6-H_2pdc (20 mM, 400 μL DMF) solution, (ii) Naphydrazide (2mM, 2500 μL DMF) and 2,6-H_2pdc (10 mM, 400 μL DMF) solution λem = 383 nm)

Figure S11 Fluorescence spectroscopic titration a solution of Naphydrazide (2.5 ml, 2mM) and 2,6-H_2pdc (20 mM, 400 μL) (λ_{ex} = 335 nm, λ_{em} = 383 nm) upon each time addition of solution of Cd^{2+} ions (50 μL of 20mM in water) and (b) changes with time after the addition of 400 μL of 20 mM Cd^{2+} ion solution .

Figure S12 Fluorescence turn-on observed in DMF solution of Naphydrazide (2 mM, 2.5 mL) together with 2,6-H_2pdc (20 mM, 400 μL) after addition of solution of Cd^{2+} ions in the presence of (a) NH_4^+ , (b) Na^+ , (c) K^+ , (d) Li^+ , (e) Cs^+ , (f) Mg^{2+}, (g) Al^{3+} , (h) Ag^+ , (i) Fe^{2+}, (j) Sn^{2+} ions (in each case 400 μL of 20 mM Cd^{2+} with 400 μL of 20 mM another ion).

Figure S13 Comparative fluorescence turn-on observed in DMF solution of Naphydrazide (2.5 mL, 2 mM) alone and in the presence of 2,6-H_2pdc (20 mM, 400 μL), Fe^{2+} and Cd^{2+} ions (metal ions, 20 mM solution water).

Figure S14 Plot of fluorescence intensity with increasing concentrations at 400 nm of a solution of Naphydrazide (2.5 mL, 2 mM) and 2,6-H_2pdc (20 mM, 400μL) upon addition of Cd^{2+} ions.

Figure S15 Fluorescence emission titration by adding 400 μL 20 mM Fe^{2+} followed by addition of 100 μL, 20 mM Cd^{2+} solution in each aliquot to (a) Naphydrazide (2mM, 2500 μL DMF) and 2,6-H_2pdc (10 mM, 400 μL DMF) and (b) Naphydrazide (2mM, 2500 μL DMF) and 2,6-H_2pdc (20 mM, 400 μL DMF)

Figure S16 Fluorescence decay profile of a bi-component solution of Naphydrizide and 2,6-H_2pdc with Cd^{2+} ions (violet line) and with Cd^{2+} and Fe^{2+} (blue line).

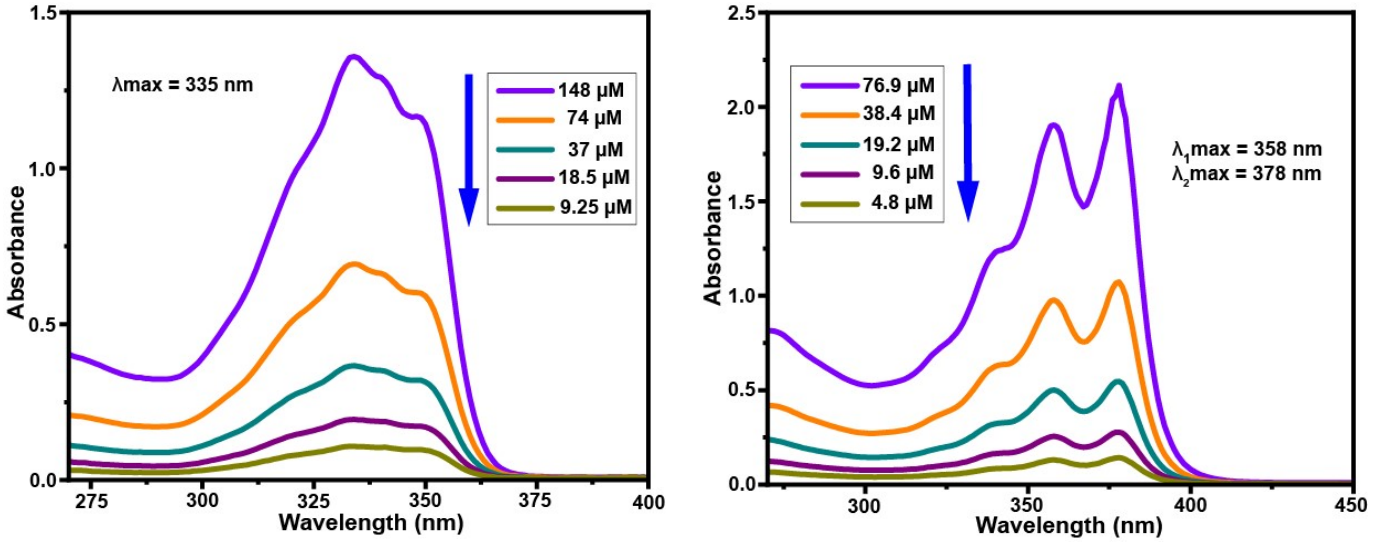

(a) (b)

Figure S1: Concentration dependent UV-visible spectra of the (a) Naphydrazide and (b) Binaphydrazide in DMF showing a decrease in absorptions upon dilution.

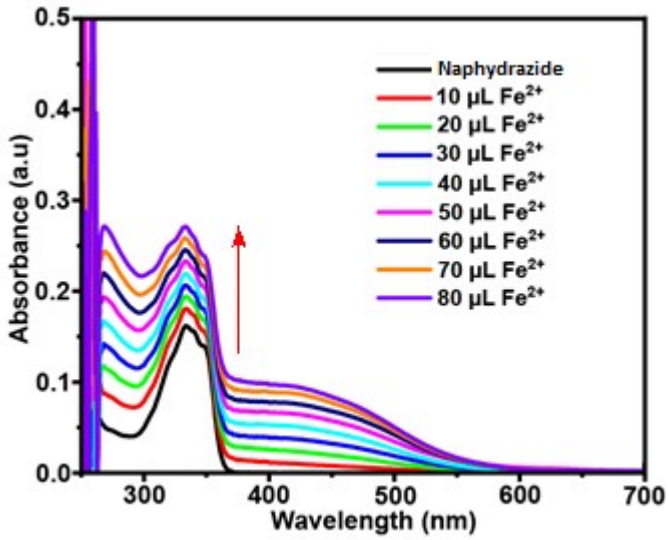

Figure S2: UV-visible titration of Naphydrazide (3.32 µM, in DMF) showing increase in the absorbance at 335 nm upon addition of Fe^{2+} ions (each time addition of 10 µL solution of 1 mM ferrous acetate in water).

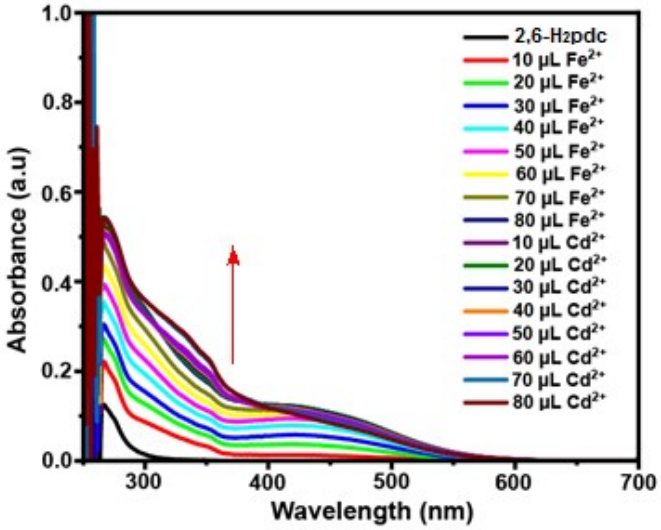

(a)

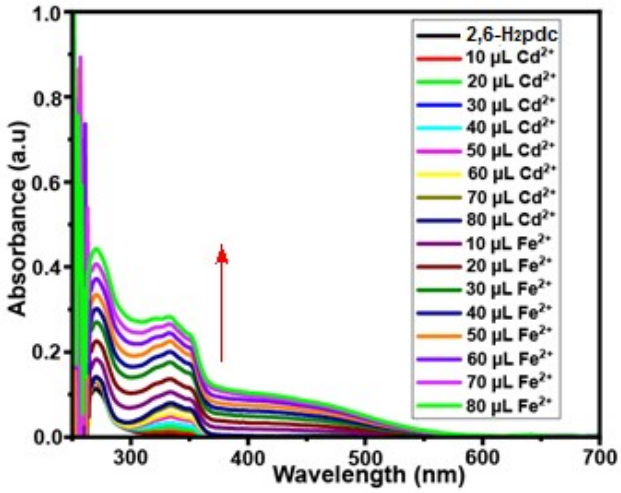

(b)

Figure S3: (a) UV-visible titration of solution of 2,6-H_2pdc (3.32 µM, 3 mL in DMF) showing increase in absorbance at 270 nm upon addition of 10-80 µL Fe^{2+} ions (1mM in water) and then addition of 10-80 µL of solution of Cd^{2+} ions (1 mM in water); (b) Same experiment by reversing the addition of the ions.

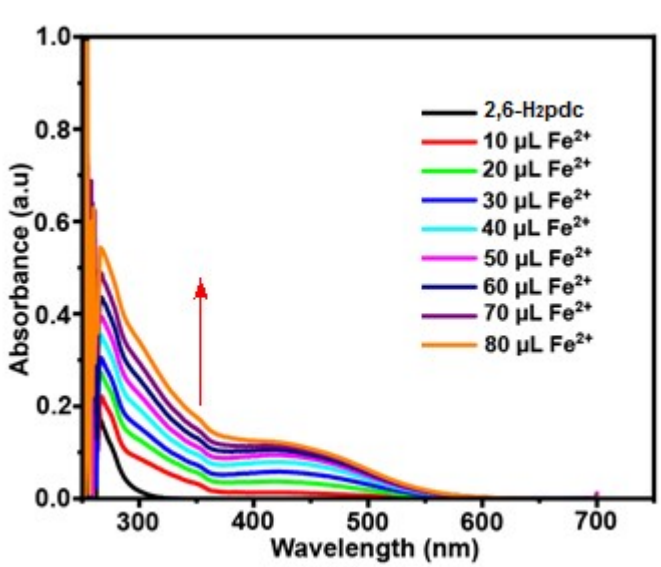

(a)

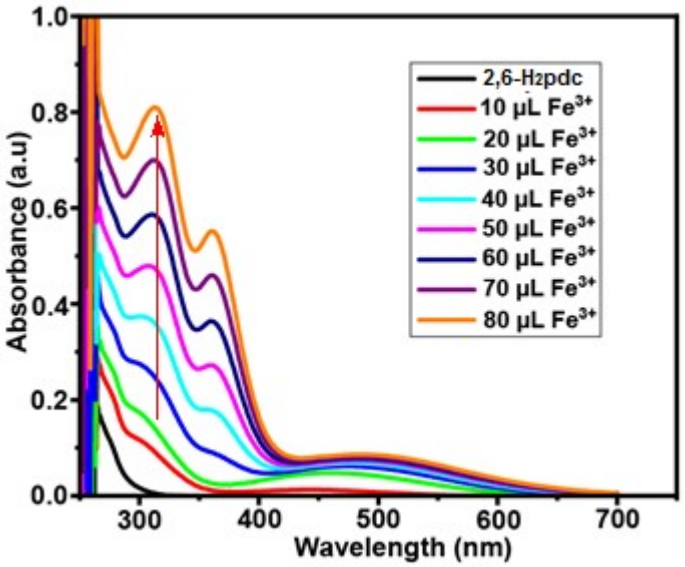

(b)

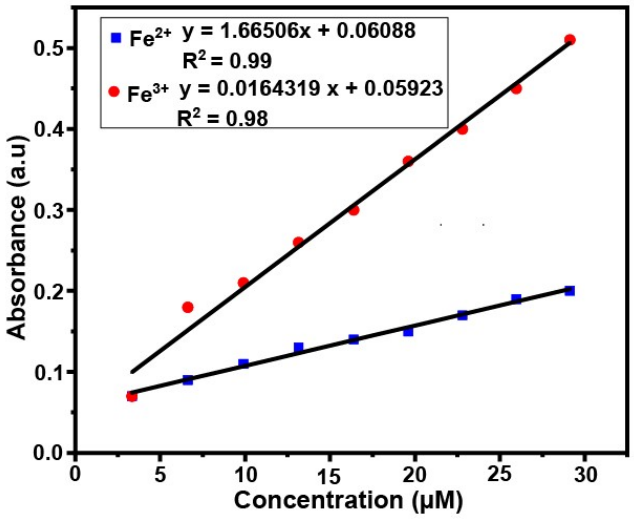

(c)

Figure S4: UV-visible titration of 2,6-H_2pdc (3.32 µM in DMF) solution with each time addition of 10 µL solution of 1 mM (a) Fe^{2+} (b) Fe^{3+} ions. (c) is the plot of concentration vs absorbance at 270 nm for Fe^{2+} and at 315 nm for Fe^{3+} of the figures (a) and (b).

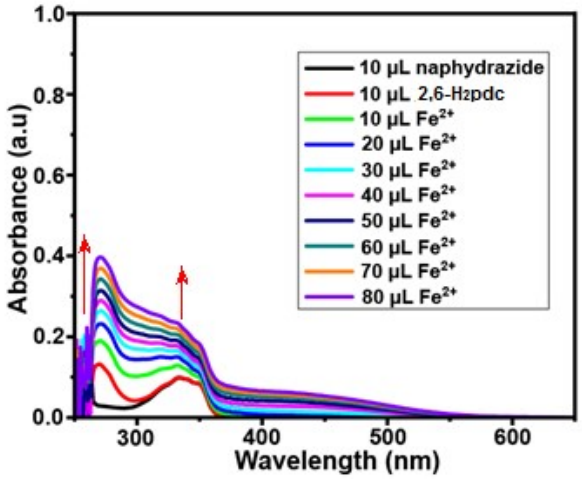

(a)

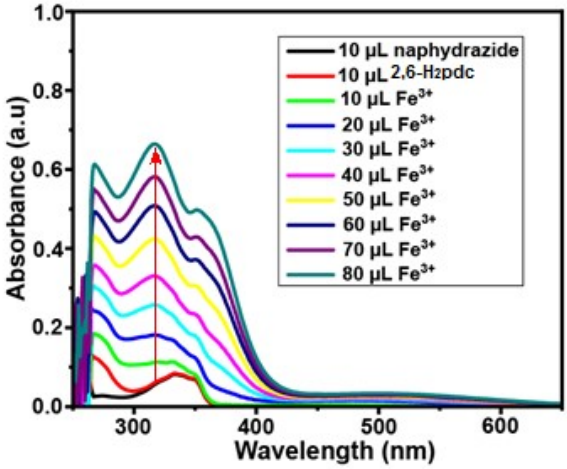

(b)

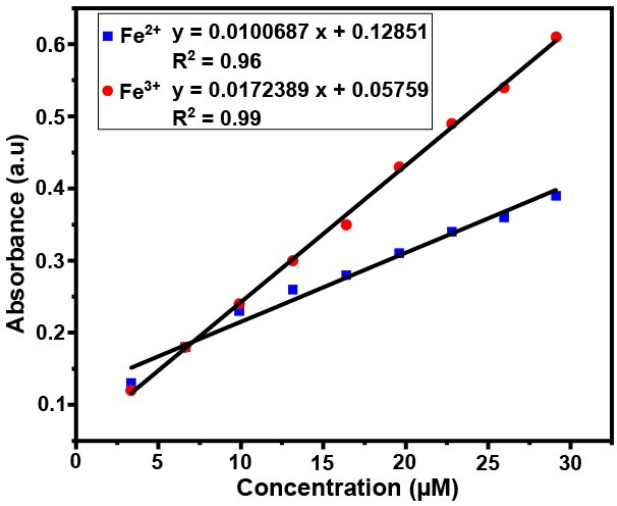

(c)

Figure S5: UV-visible titrations of a solution of Naphydrazide together with 2,6-H_2pdc (both 10 µL from 3.32 µM stock solution in DMF added to 2mL DMF) upon addition of (a) Fe^{2+} (b) Fe^{3+} ions (10 µL in each aliquot from 1 mM stock solution in water in each case) (c) Concentration dependent absorption at 270 nm from (a) and 315 nm from (b).

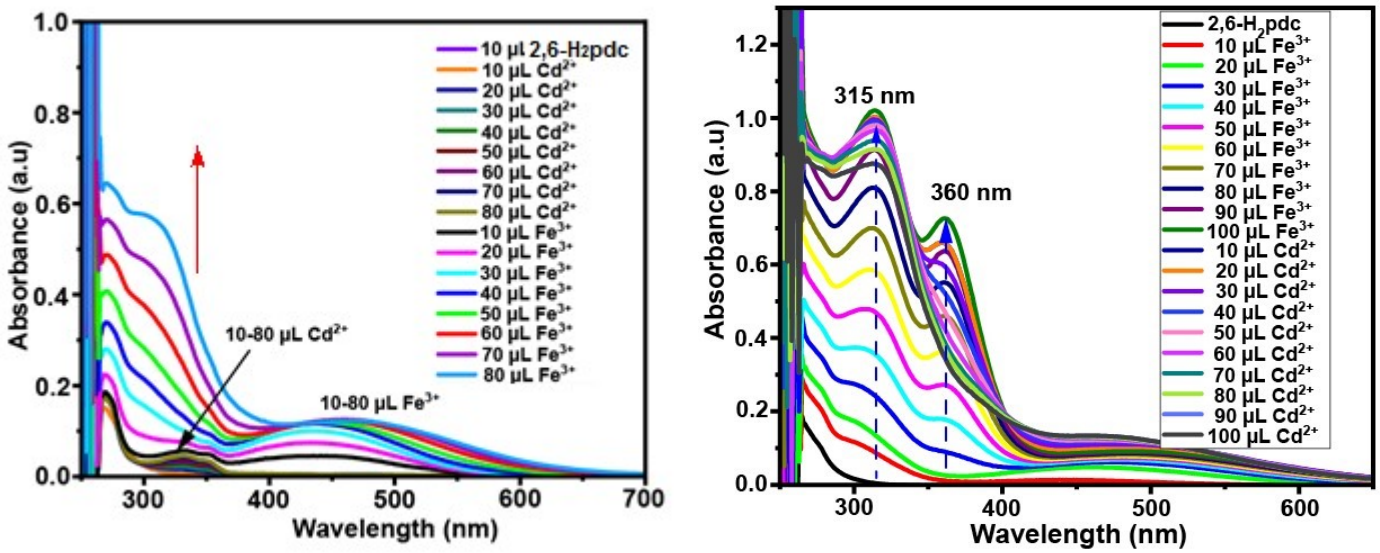

(a) (b)

Figure S6: (a) UV-visible titration of solution of 2,6-H_2pdc (3.32 µM, mL, in DMF) upon addition of 10-80 µL of solution of Cd^{2+} ions (1mM in water) insignificant changes were observed, followed by addition of 10-80 µL Fe^{3+} ions (1mM in water) caused initial increase at 270 nm, 315 nm and 450 nm and then the peak at 450 shifting to 480 nm;; (b) Same experiment by reversing the addition of the ions showing increase in absorption at 315 nm and at 360 nm with Fe^{3+} concentration, whereas upon addition of Cd^{2+} ions the intensity of the peak at 360 nm disappeared.

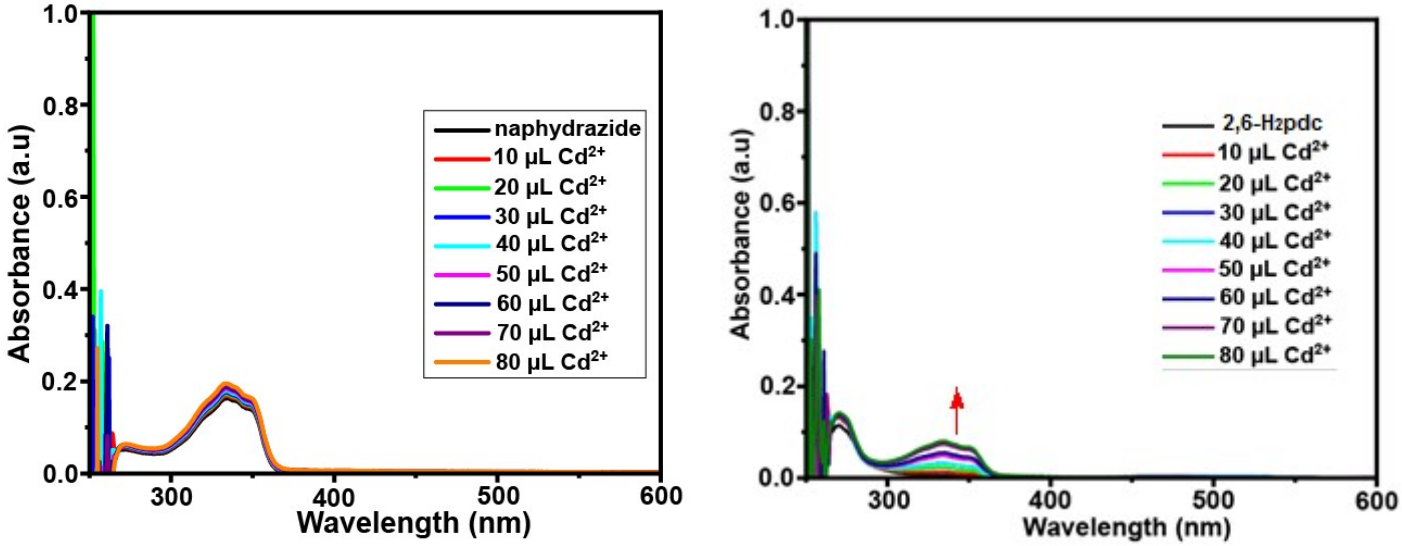

(a) (b)

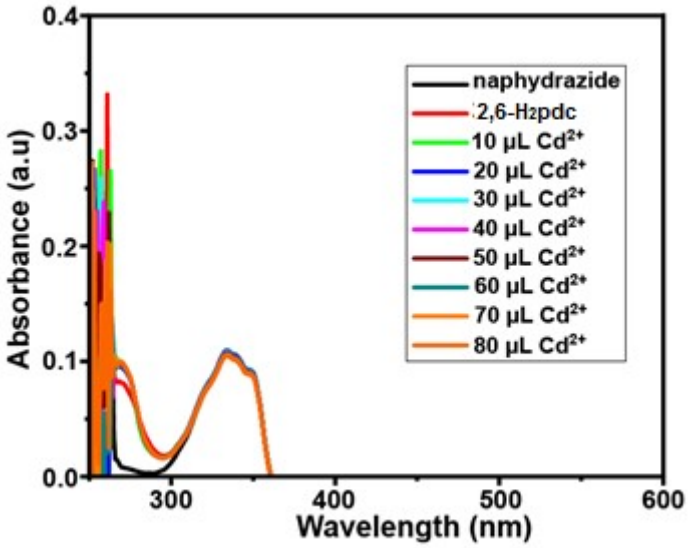

(c)

Figure S7: UV-visible titrations of (a) Naphydrazide, (b) 2,6-H_2pdc, (c) mixture of Naphydrazide and 2,6-H_2pdc, with each addition of 10 µL solution of Cd^{2+} ions (In each case the 3.32 µM of the respective compound in DMF solution; 1 mM Cd^{2+} ions in water).

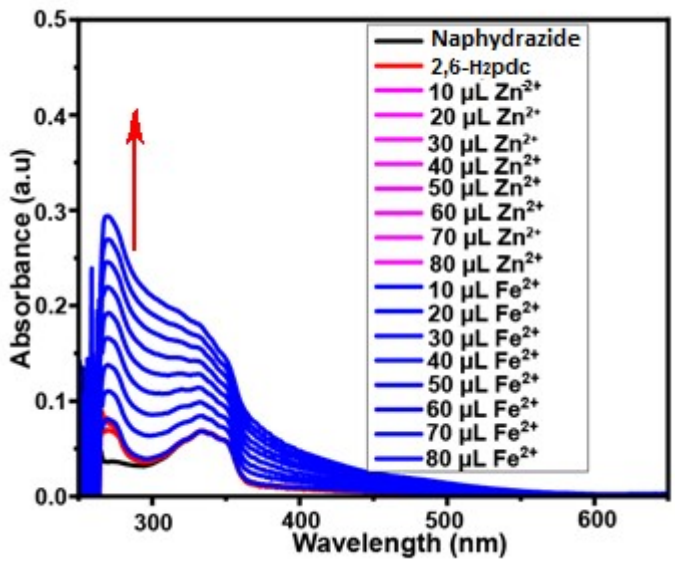

(a)

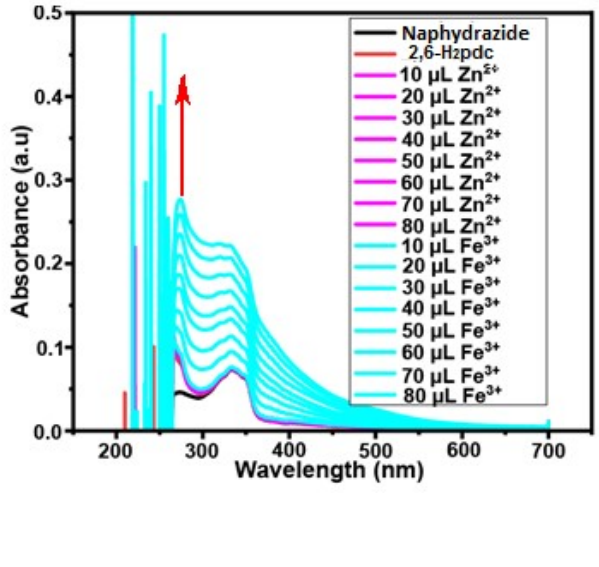

(b)

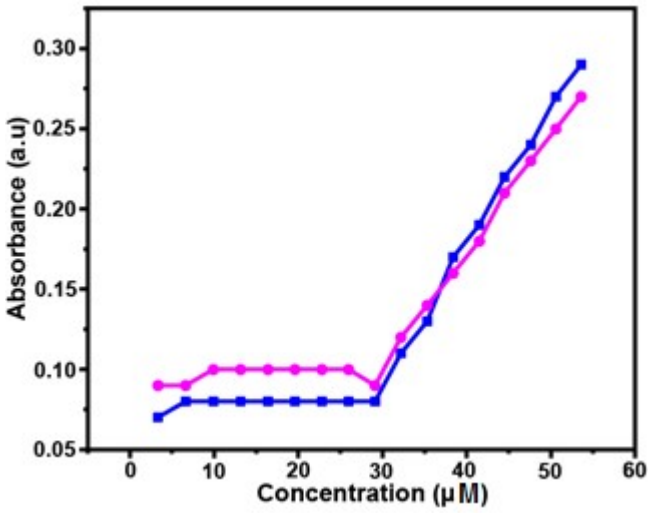

(c)

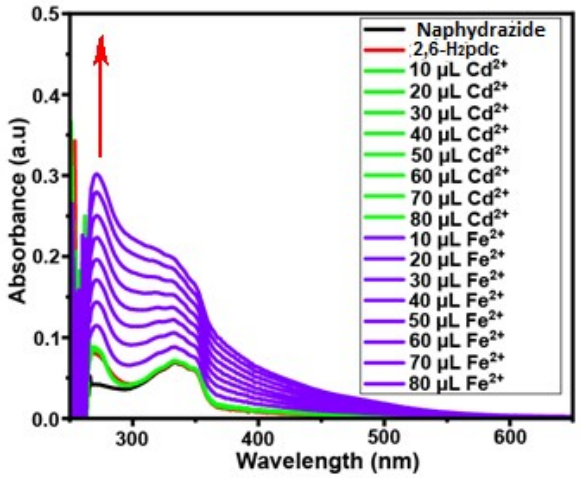

(d)

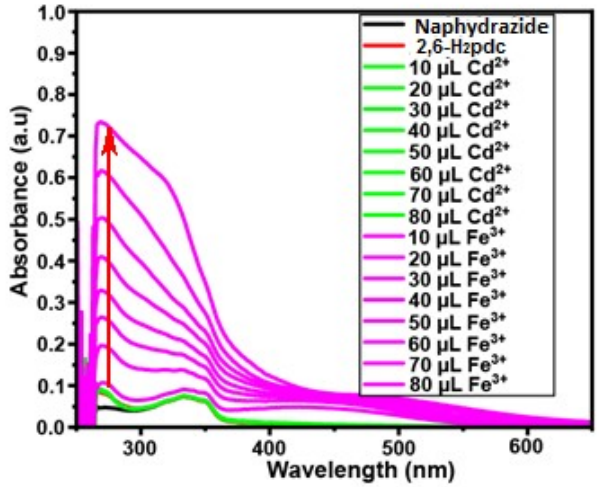

(e)

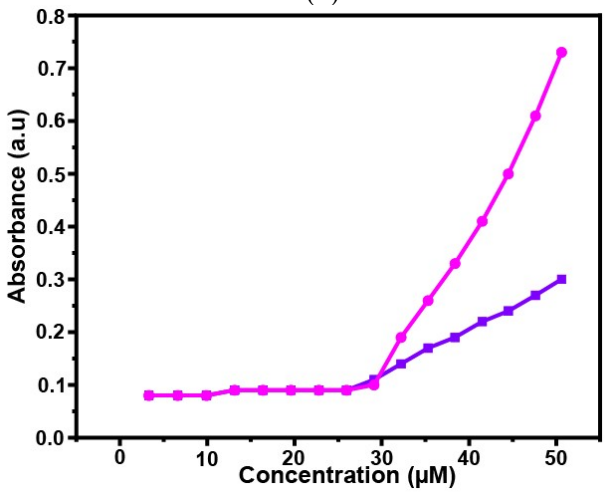

(f)

Figure S8: UV-visible titration of (a) Naphydrazide (3 mL) and 2,6-H_2pdc (0.8 mL) (taken together from respective 3.32 μM stock solution in DMF) with each aliquot addition of Zn^{2+} ions followed by addition of (a) Fe^{3+} ions and (b) Fe^{3+} ions (c) Plots of increase in the absorbance at 270 nm of a solution of the above solutions. (d) UV-visible titration of Naphydrazide (3 mL) and 2,6-H_2pdc (0.8 mL) (taken together from respective 3.32 μM stock solution in DMF) with different aliquots of solution of Cd^{2+} ions followed by (d) Fe^{3+} ions and (e) Fe^{2+} ions; (e) The plots of absorbances at 270 nm against concentration of ions from the figures (d) and (e).

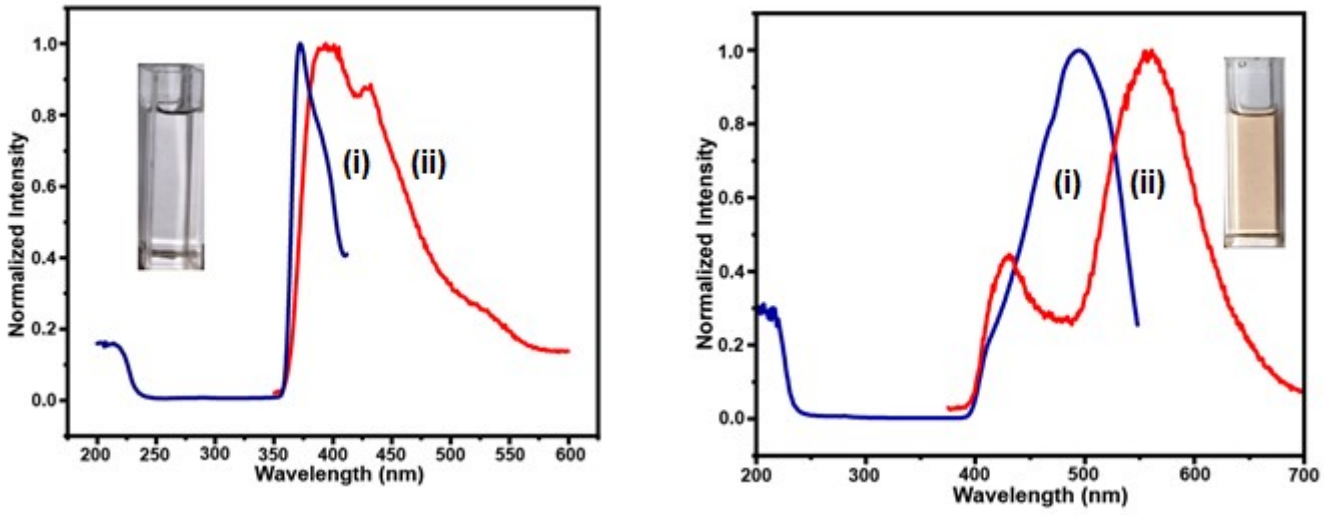

(a) (b)

Figure S9: Fluorescence excitation (i) and emission spectra (ii) of (a) Naphydrazide (λ_{ex} = 335 nm, λ_{em} = 396 nm) (b) Binaphydrazide (λ_{ex} = 378 nm, λ_{em} = 558 nm) in DMF (3mL of 2mM solution of receptor in each case).

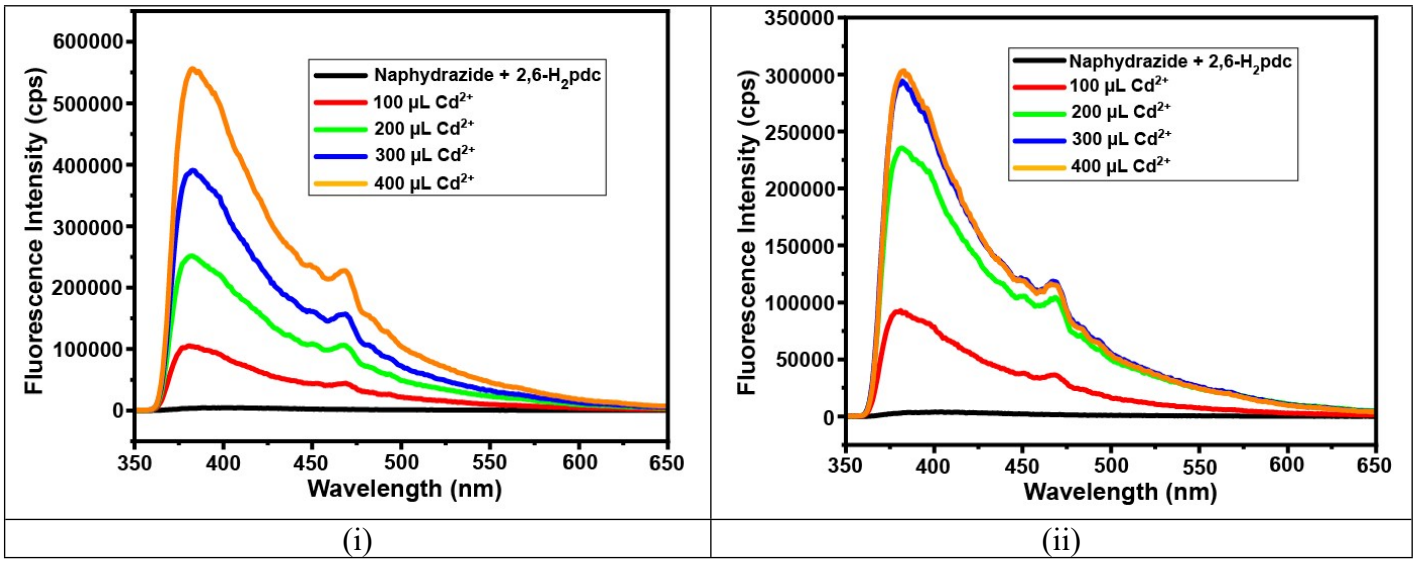

(i) (ii)

Figure S10: Fluorescence emission titration by adding100 µL, 20 mM Cd^{2+} solution followed by addition of aliquots of 100 µL, 20 mM Cd^{2+} solution to (i) Naphydrazide (2mM, 2500 µL DMF) and 2,6-H_2pdc (20 mM, 400 µL DMF) solution, (ii) Naphydrazide (2mM, 2500 µL DMF) and 2,6-H_2pdc (10 mM, 400 µL DMF) solution λem = 383 nm)

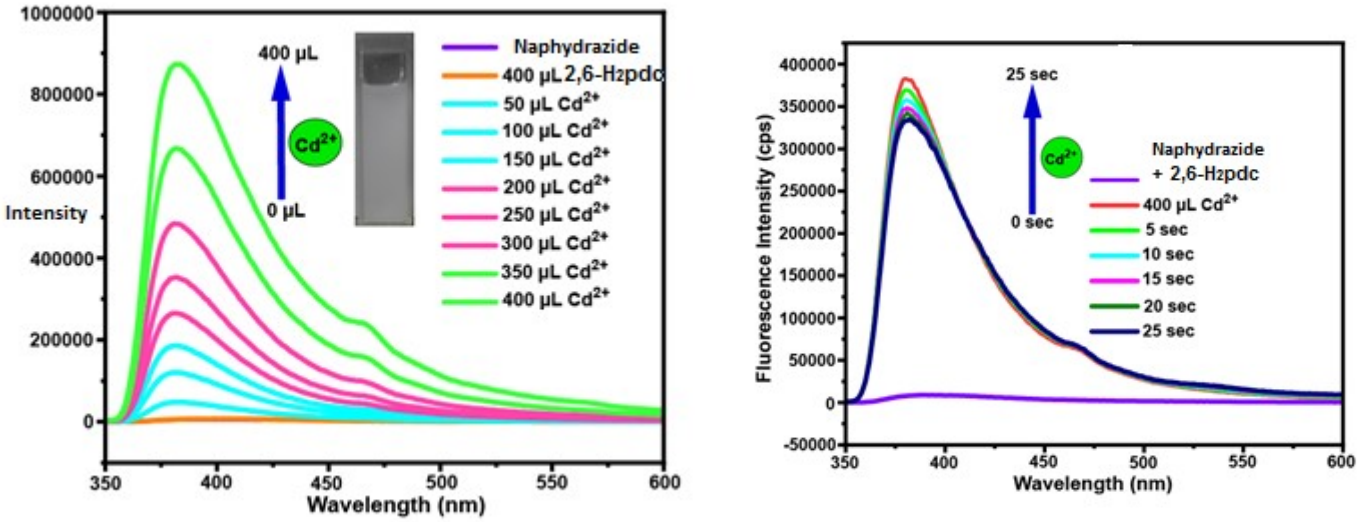

(a) (b)

Figure S11: Fluorescence spectroscopic titration a solution of Naphydrazide (2.5 ml, 2mM) and 2,6-H_2pdc (20 mM, 400 µL) (λ_{ex} = 335 nm, λ_{em} = 383 nm) upon each time addition of solution of Cd^{2+} ions (50 µL of 20mM in water) and (b) changes with time after the addition of 400 µL of 20 mM Cd^{2+} ion solution .

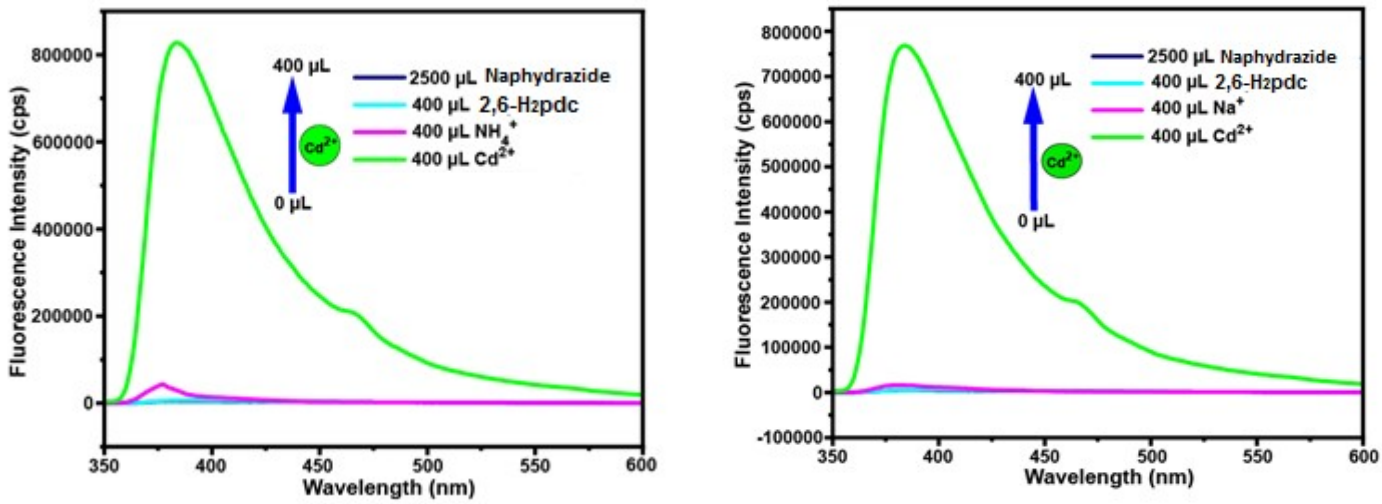

(a) (b)

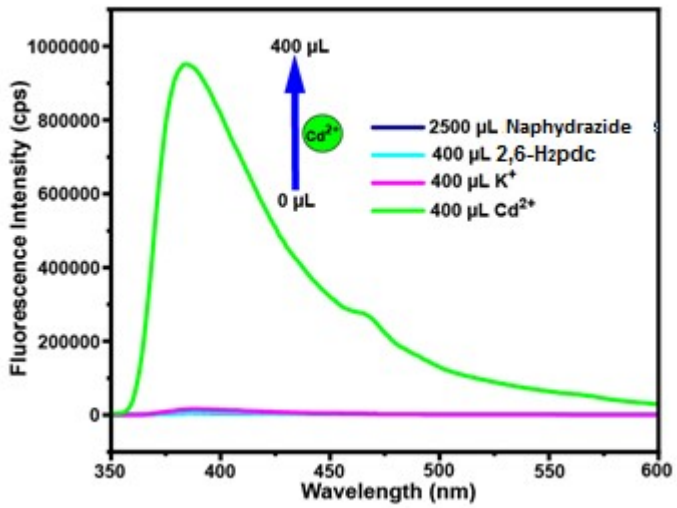
Fluorescence Intensity (cps)
Wavelength (nm)
400 µL
0 µL
Cd2+
2500 µL Naphydrazide
400 µL 2,6-H2pdc
400 µL K+
400 µL Cd2+

(c)

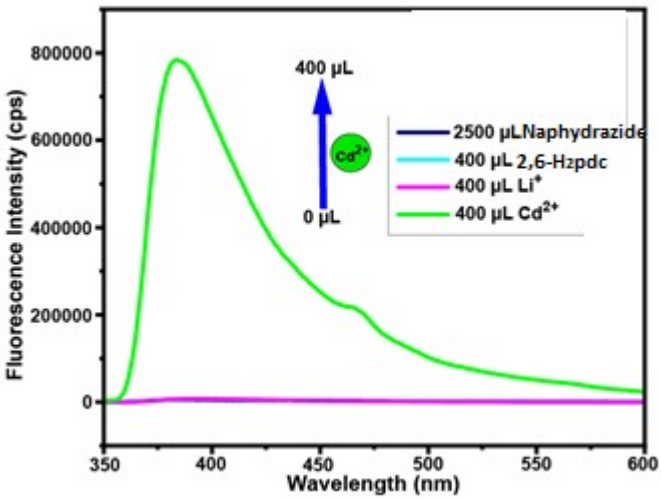
Fluorescence Intensity (cps)
Wavelength (nm)
400 µL
0 µL
Cd2+
2500 µLNaphydrazide
400 µL 2,6-H2pdc
400 µL Li+
400 µL Cd2+

(d)

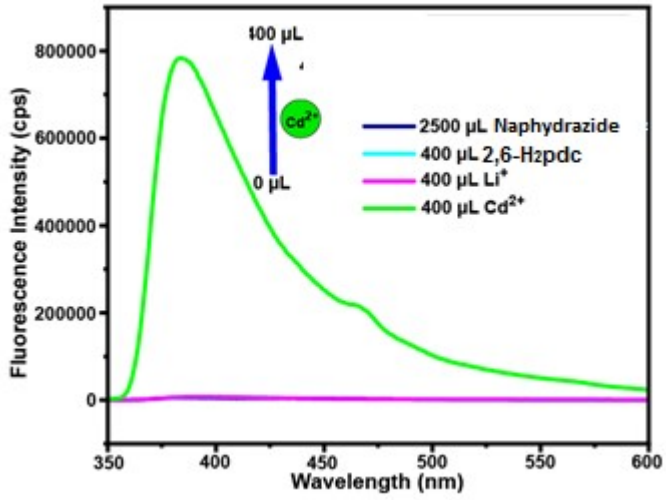
Fluorescence Intensity (cps)
Wavelength (nm)
100 µL
0 µL
Cd2+
2500 µL Naphydrazide
400 µL 2,6-H2pdc
400 µL Li+
400 µL Cd2+

(e)

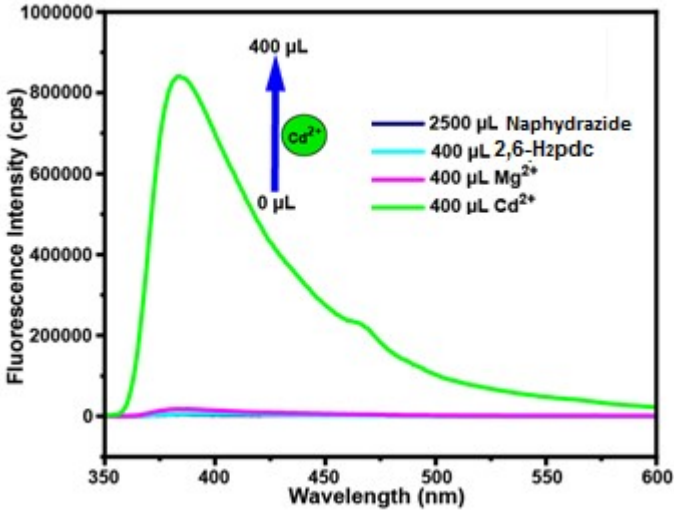
Fluorescence Intensity (cps)
Wavelength (nm)
400 µL
0 µL
Cd2+
2500 µL Naphydrazide
400 µL 2,6-H2pdc
400 µL Mg2+
400 µL Cd2+

(f)

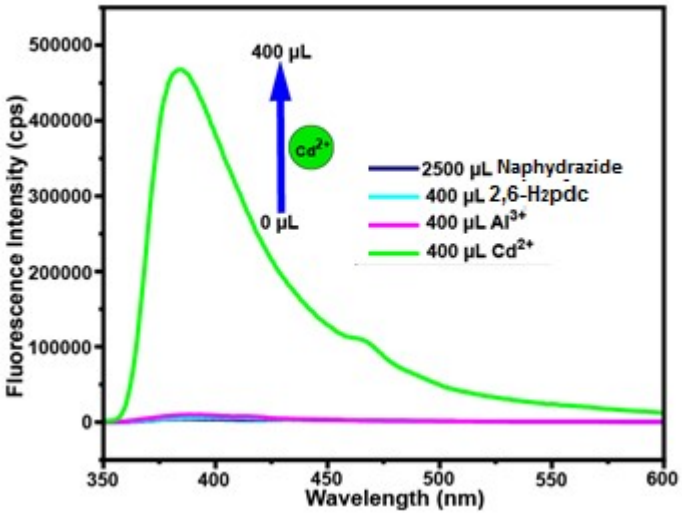
Fluorescence Intensity (cps)
Wavelength (nm)
400 µL
0 µL
Cd2+
2500 µL Naphydrazide
400 µL 2,6-H2pdc
400 µL Al3+
400 µL Cd2+

(g)

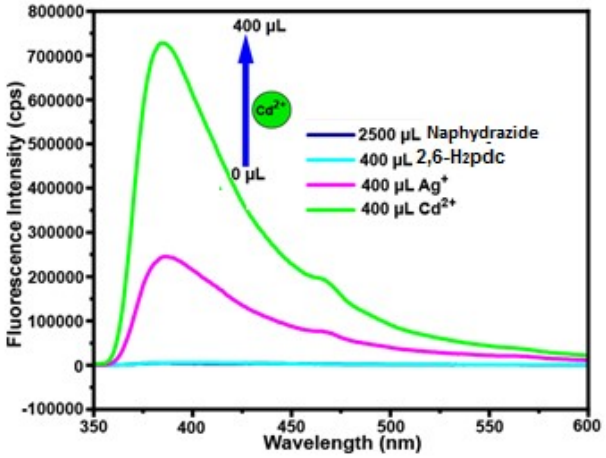
Fluorescence Intensity (cps)
Wavelength (nm)
400 µL
0 µL
Cd2+
2500 µL Naphydrazide
400 µL 2,6-H2pdc
400 µL Ag+
400 µL Cd2+

(h)

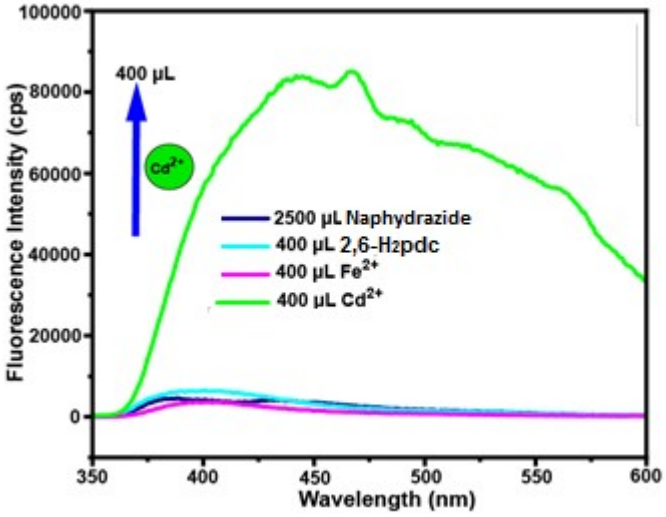

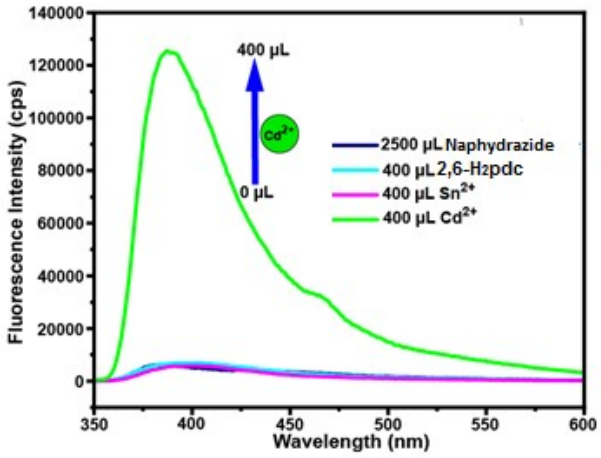

(i) (j)

Figure S12: Fluorescence turn-on observed in DMF solution of Naphydrazide (2 mM, 2.5 mL) together with 2,6-H_2pdc (20 mM, 400 µL) after addition of solution of Cd^{2+} ions in the presence of (a) NH_4^+ , (b) Na^+ , (c) K^+ , (d) Li^+ , (e) Cs^+ , (f) Mg^{2+}, (g) Al^{3+} , (h) Ag^+ , (i) Fe^{2+}, (j) Sn^{2+} ions (in each case 400 µL of 20 mM Cd^{2+} with 400 µL of 20 mM another ion).

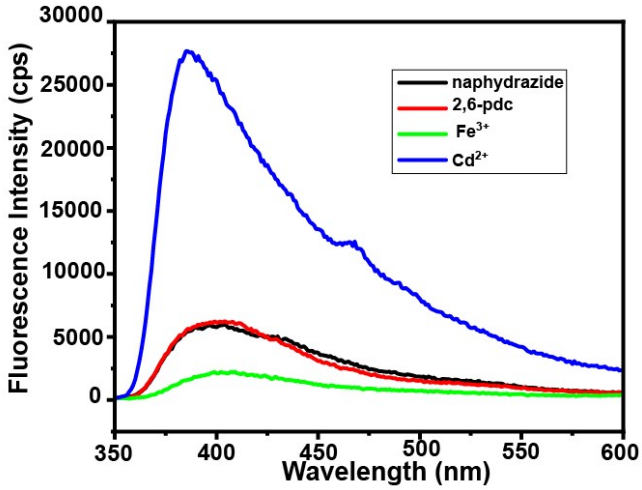

Figure S13: Comparative fluorescence turn-on observed in DMF solution of Naphydrazide (2.5 mL, 2 mM) alone and in the presence of 2,6-H_2pdc (20 mM, 400 µL), Fe^{2+} and Cd^{2+} ions (metal ions, 20 mM solution water).

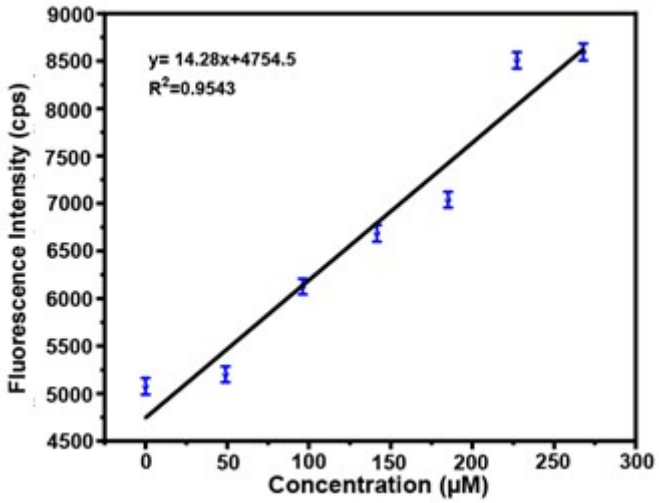

Figure S14: Plot of fluorescence intensity with increasing concentrations at 400 nm of a solution of Naphydrazide (2.5 mL, 2 mM) and 2,6-H_2pdc (20 mM, 400μL) upon addition of Cd^{2+} ions.

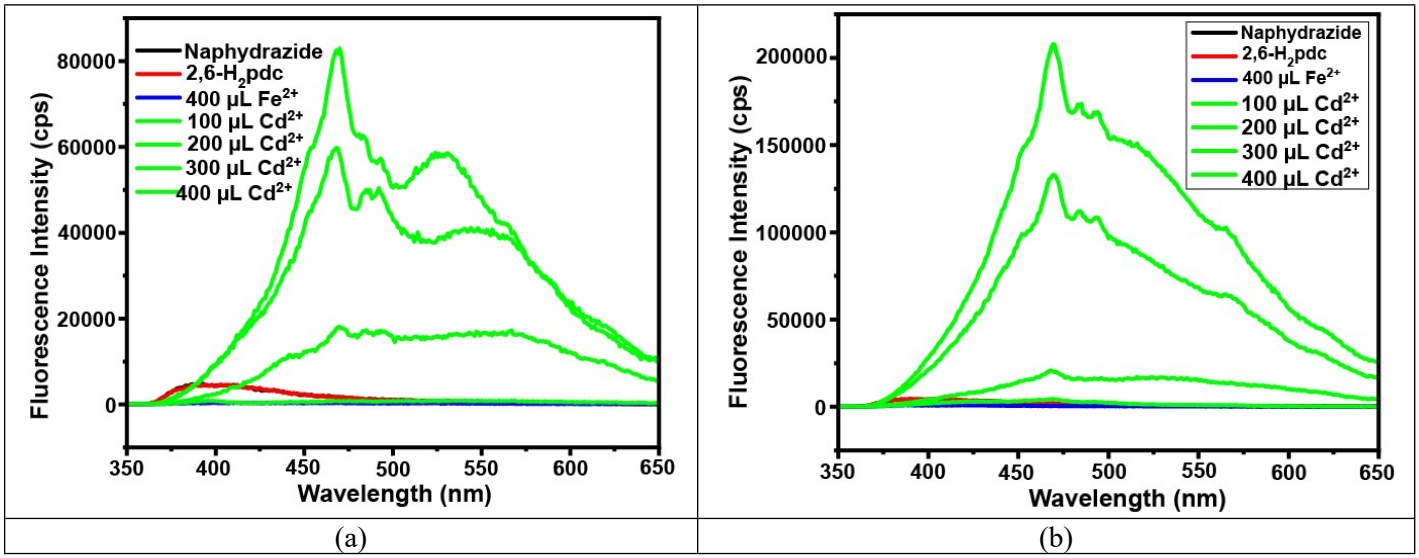

(a) (b)

Figure S15: Fluorescence emission titration by adding 400 μL 20 mM Fe^{2+} followed by addition of 100 μL, 20 mM Cd^{2+} solution in each aliquot to (a) Naphydrazide (2 mM, 2500 μL DMF) and 2,6-H_2pdc (10 mM, 400 μL DMF) and (b) Naphydrazide (2mM, 2500 μL DMF) and 2,6-H_2pdc (20 mM, 400 μL DMF)

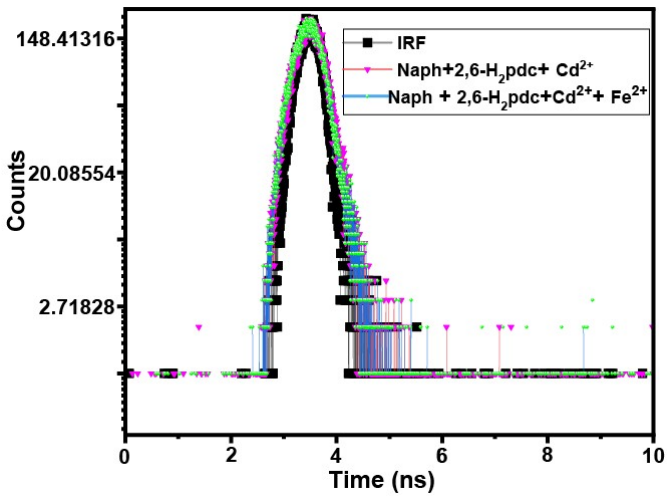

❖ **Exponential Components Analysis (Tail Fitting)**

Fitting range : [1439; 2200] channels
χ^2 : 1.052

	B_i	ΔB_i	f_i (%)	Δf_i (%)	τ_i (ns)	$\Delta\tau_i$ (ns)
1	-158.3056	6.6835	10.424	0.440	0.050 fixed	0
2	301.7336	3.8243	89.576	17.483	0.225	0.041

Shift : 0 ns (± 0 ns)
Decay Background : -0.160 (± 0.125)

❖ **Exponential Components Analysis (Tail Fitting)**

Fitting range : [1404; 2200] channels
χ^2 : 1.046

	B_i	ΔB_i	f_i (%)	Δf_i (%)	τ_i (ns)	$\Delta\tau_i$ (ns)
1	-424.5000	15.0186	27.027	0.956	0.100 fixed	0
2	565.2792	12.7721	72.973	20.270	0.203	0.052

Shift : 0 ns (± 0 ns)
Decay Background : 0.147 (± 0.124)

Figure S16 : Fluorescence decay profile of a bi-component solution of Naphydrizide and 2,6-H_2pdc with Cd^{2+} ions (violet line) and with Cd^{2+} and Fe^{2+} (blue line).The data for the without Fe^{2+} is on left and right is with Fe^{2+}.

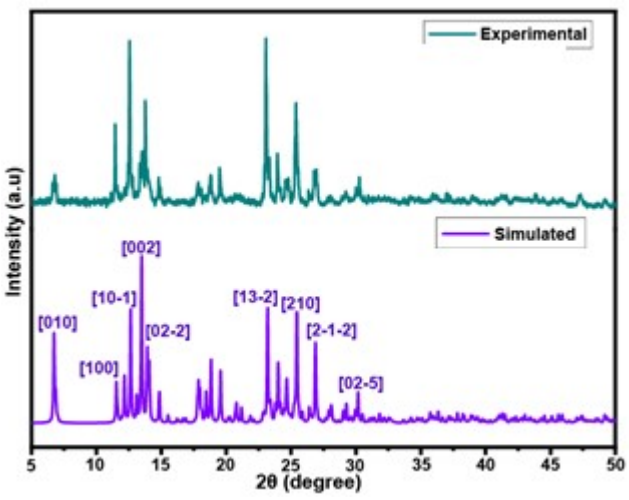

(i)

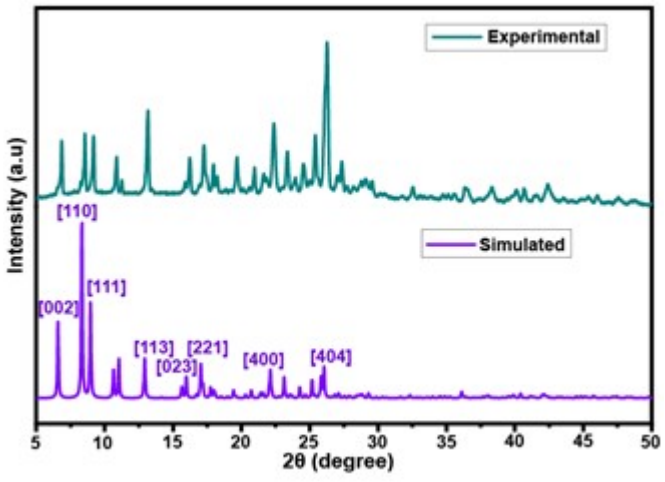

(ii)

Figure S17: Experimental and Simulated stacking powder XRD pattern of (i) [(HNaphydrazide)[Fe(2,6-pdc)$_2$]·H_2O (ii) [(H_2Binaphydrazide)[Fe(2,6-pdc)$_2$]$_2$ ·4.5H_2O.

(a) (b)

Figure S18: Optical microscopic images of the complex (a) [(HNaphydrazide)[Fe(2,6-pdc)$_2$]·H_2O and (b) [(H_2 Binaphydrazide)[Fe(2,6-pdc)$_2$]$_2$·4.5H_2O.

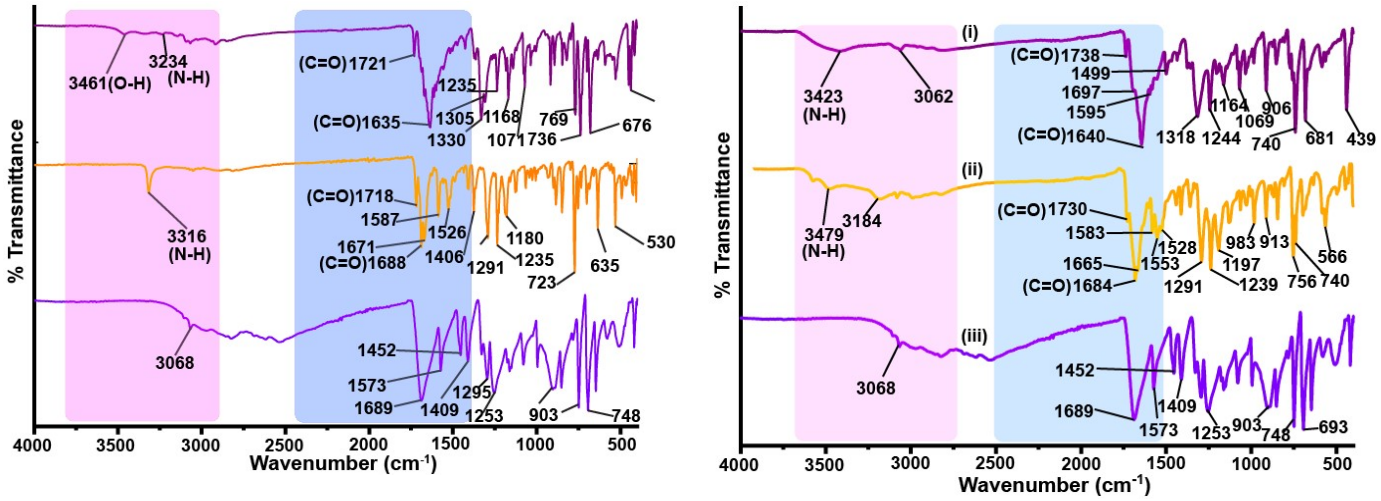

(a) (b)

Figure S19: FTIR spectra powder samples of complex (a) [(HNaphydrazide)[Fe(2,6-pdc)$_2$]·H_2O and (b) [(H_2 Binaphydrazide)[Fe(2,6-pdc)$_2$]$_2$·4.5H_2O.

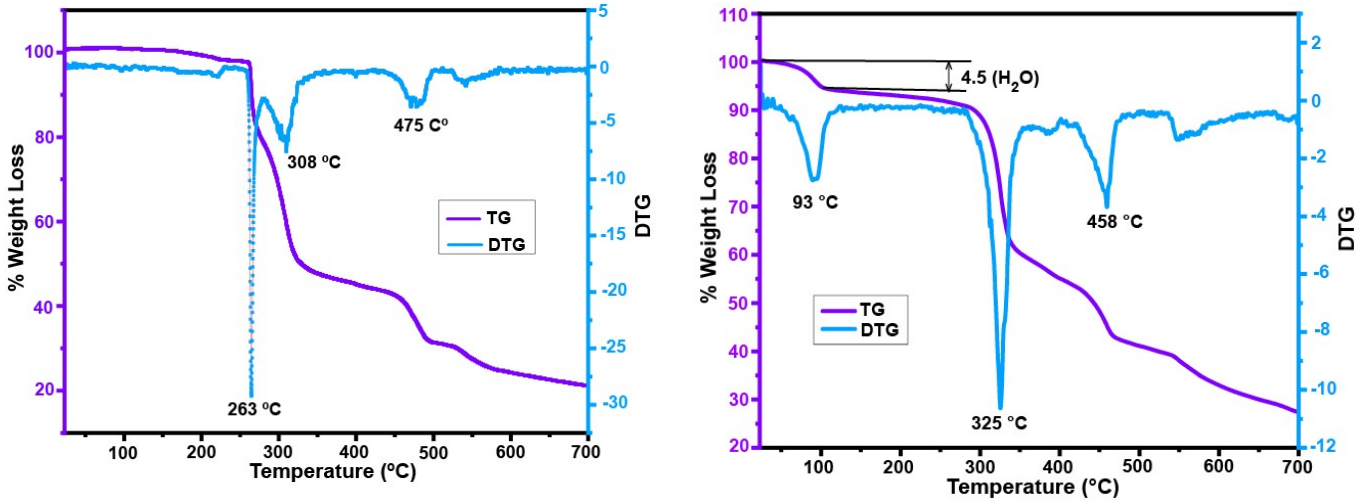

(a) (b)

Figure S20: Thermogram of the complex (a) [(HNaphydrazide)[Fe(2,6-pdc)$_2$]·H_2O, and (b) [(H_2 Binaphydrazide)[Fe(2,6-pdc)$_2$]$_2$ ·4.5H_2O in argon environment with heating rate 10 °C/min.

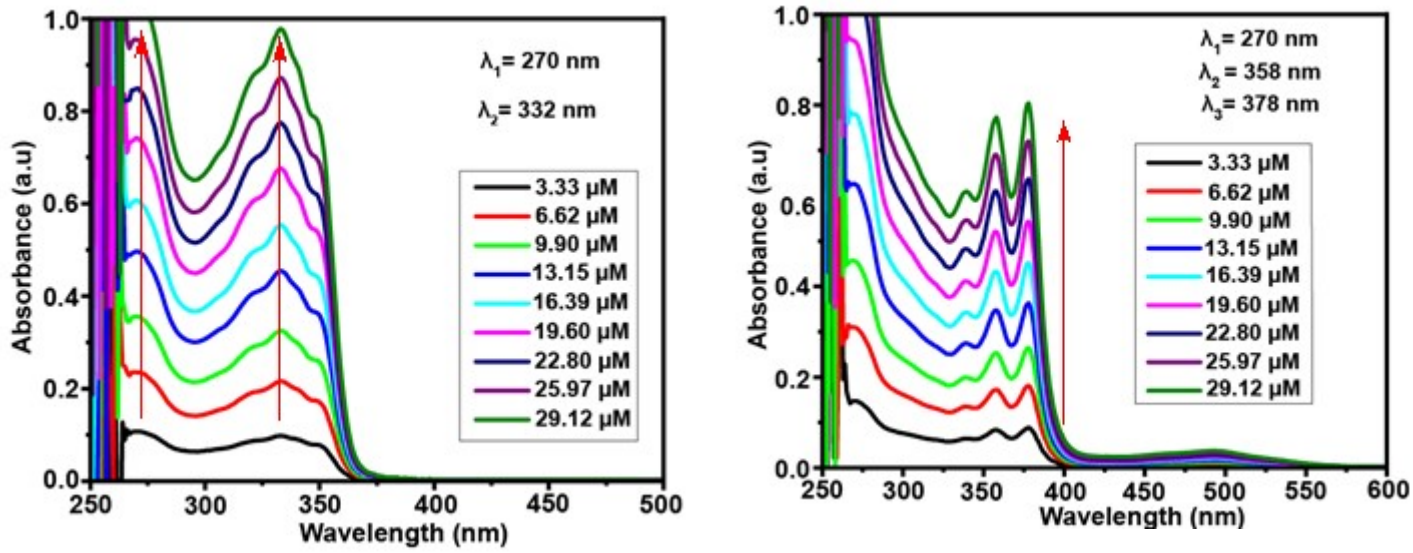

(a) (b)

Figure S21: UV-visible spectra of the (a) [(HNaphydrazide)[Fe(2,6-pdc)$_2$]·H_2O and (b) [(H_2Binaphydrazide) [Fe(2,6-pdc)$_2$]$_2$·4.5H_2O (solution in different concentrations in DMF).

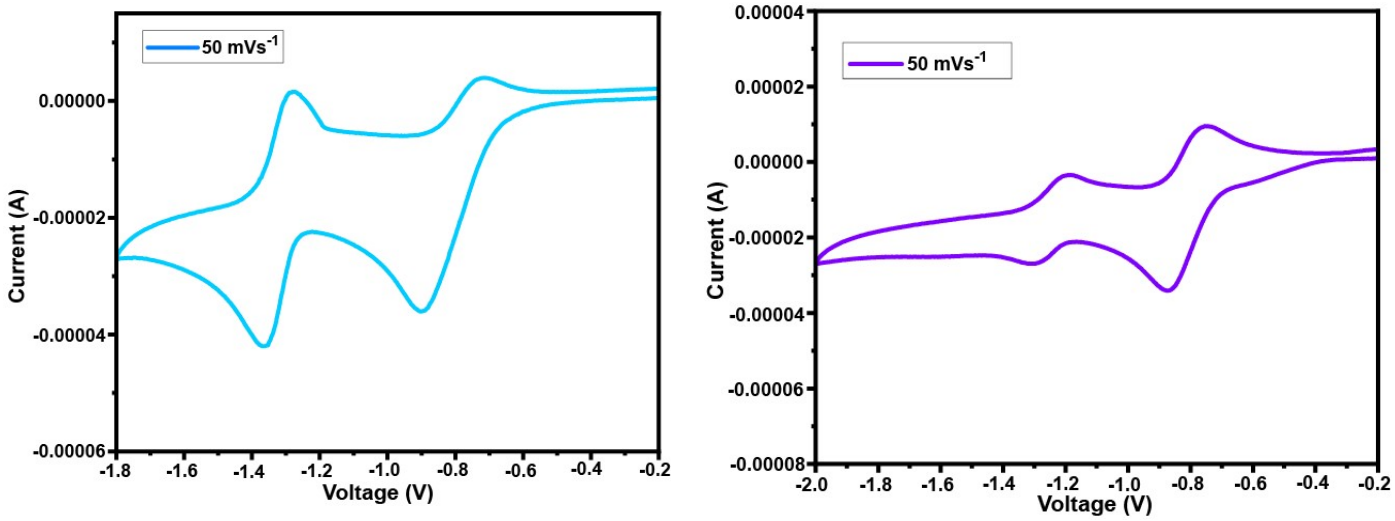

(a) (b)

Figure S22: Cyclic-voltamogram of the (a) Naphydrazide and (b) Binaphydrazide (solution in DMF with scan rate of 50 mVs^{-1})

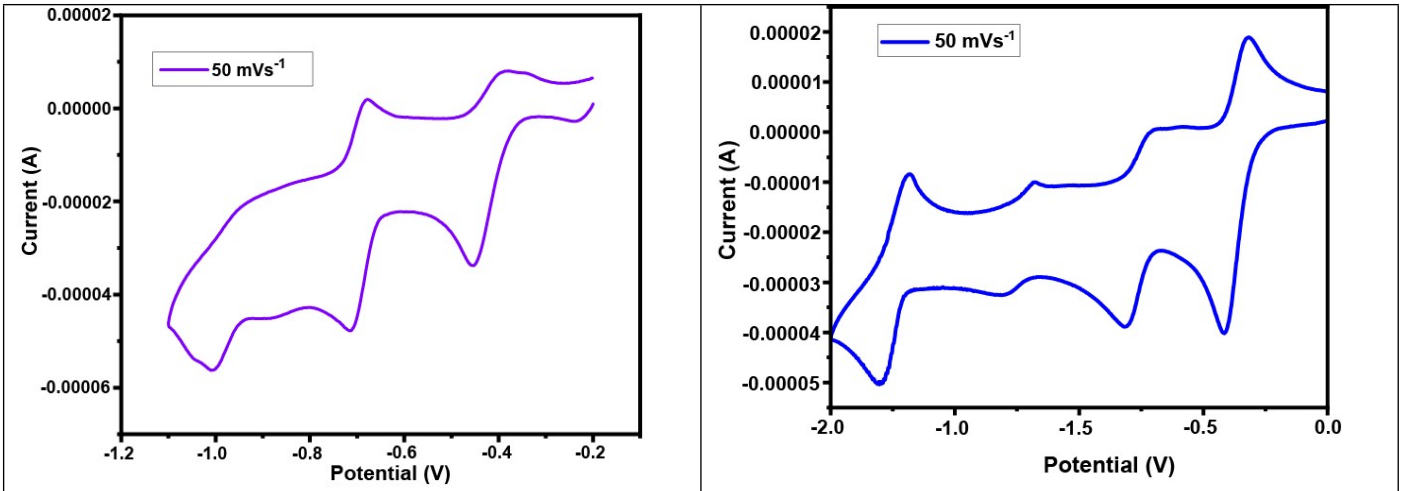

(i) (ii)

Figure S23: Cyclic-voltamogram of the compounds (a) $[(HNaphydrazide)[Fe(2,6\text{-}pdc)_2]\cdot H_2O$ and (b) $[(H_2Binaphydrazide)[Fe(2,6\text{-}pdc)_2]_2\cdot 4.5H_2O$ in DMF (scan rate of 50 mVs^{-1}).

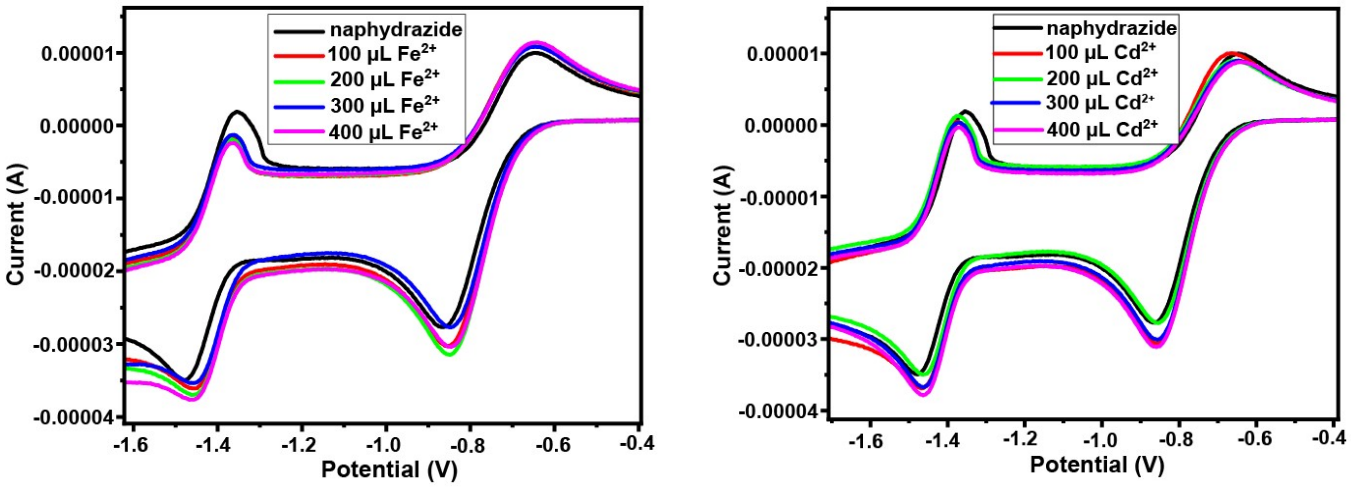

(a) (b)

Figure S24: Cyclic-voltamometric titrations of solution of (a) Naphydrazide in DMF (1 mM) with each addition of 100 µL solution of Fe^{2+} ions (1 mM In water) (b) Naphydrazide (31 mM in DMF) solution with each time addition of 100 µL solution of Cd^{2+} ions (1 mM in water).

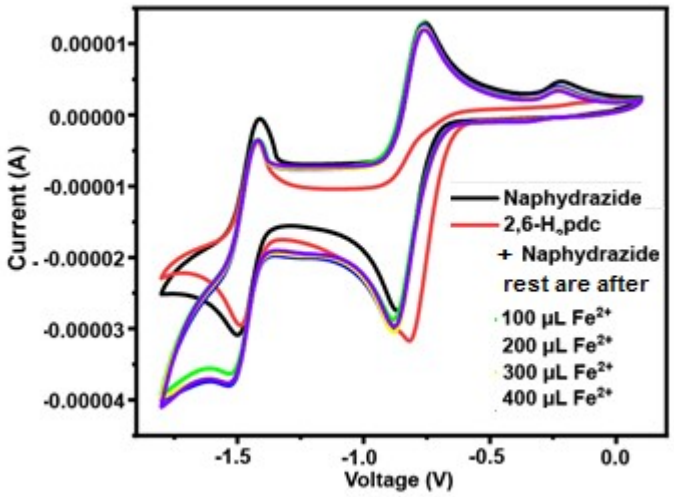

Figure S25: Cyclic-voltametric titration of Naphydrazide and 2,6-H_2pdc (1mM, 10 mL of each) in DMF to which solution of Fe^{2+} ions was added (100 µL solution in different aliquots from a 1 mM solution of the corresponding stock solution of the metal ion).

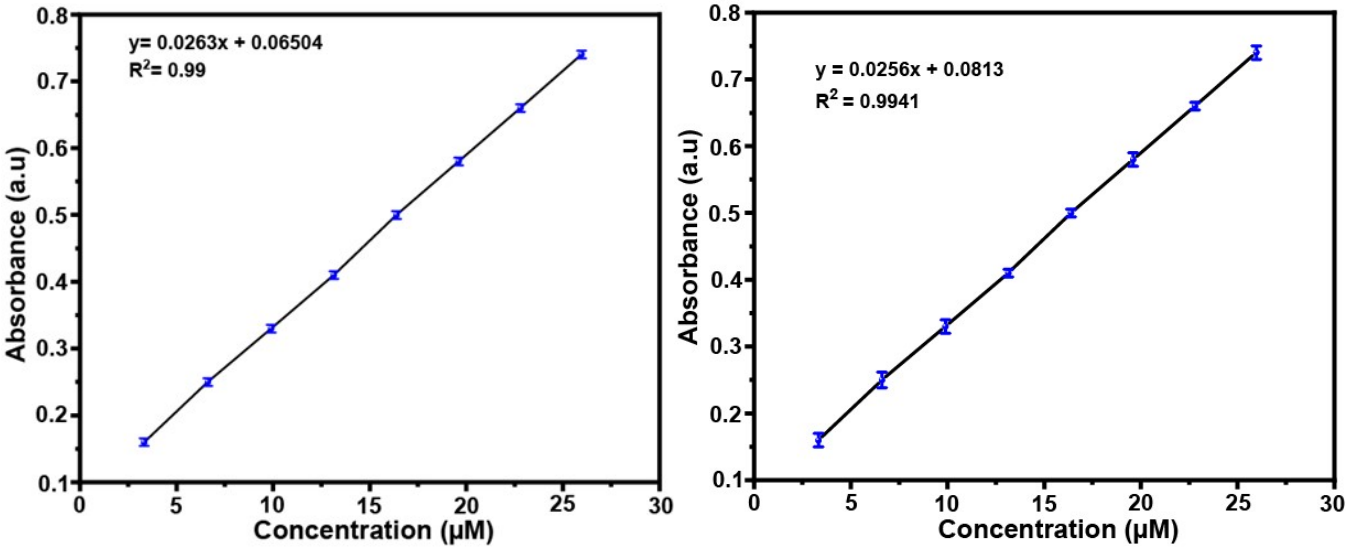

(a)

(b)

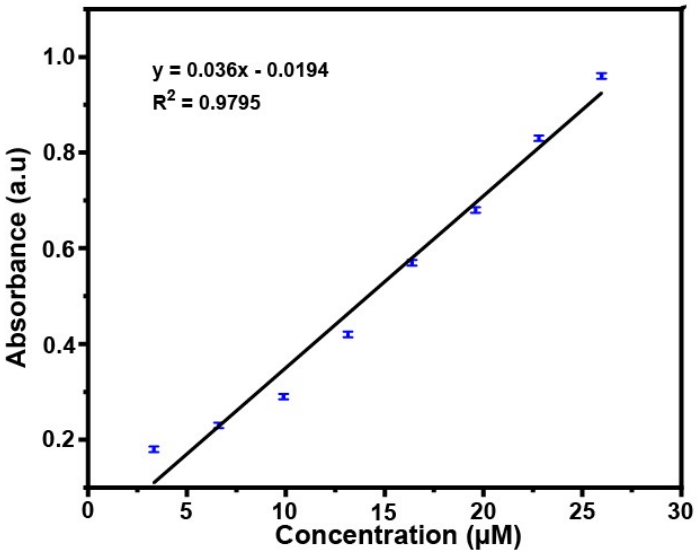

(c)

Figure S26: Plots of the changes in the intensity of absorptions of solutions of (a) Naphydrazide and 2,6-H_2pdc concentration (b) 2,6-H_2pdc and (c) Naphhydrazide upon addition of Fe^{3+} (Used for determining limit of detections).

Table S1 : The E_{pc}, E_{pa} and $E_{1/2}$ values observed in cyclic-voltamogram

Compound/complex	E_{pc}/V	E_{pa}/V	$E_{1/2}$/V
Naphydrazide	-0.713 and -1.364	-0.902 and -1.279	-0.807 and -1.321
Binaphydrazide	-0.753 and -1.189	-0.876 and -1.304	-0.815 and -1.247
[(HNaphydrazide)[Fe(2,6-pdc)$_2$]·H_2O	-0.455, -0.715	-0.380, -0.679 and -1.02	-0.418 and -0.697
[(H_2Binaphydrazide)[Fe(2,6-pdc)$_2$]$_2$·4.5H_2O	-0.319, -0.714 and -1.688	-0.414, -0.818 and-1.800	-0.367, -0.766 and -1.744

Table S2: Metal-ligand bond-angles and bond-distances in the two complexes

[(HNaphydrazide)[Fe(2,6-pdc)$_2$]·H_2O			
Bond-length (Å)		Bond angle (°)	
Fe1-O10	1.998(19)	O10-Fe1-O9	150.68(6)
Fe1-O9	2.015(2)	O10-Fe1-O6	94.68(8)
Fe1-O6	2.025(2)	O9-Fe1-O6	94.36(8)
Fe1-O5	2.037(2)	O10-Fe1-O5	94.14(7)
Fe1-N4	2.064(2)	O9-Fe1-O5	91.36(8)
Fe1-N5	2.071(2)	O6-Fe1-O5	150.87(7)
		O10-Fe1-N4	116.14(8)
		O9-Fe1-N4	93.12(8)
		O6-Fe1-N4	75.76(8)
		O5-Fe1-N4	75.43(7)
		O10-Fe1-N5	75.35(9)
		O9-Fe1-N5	75.33(8)
		O6-Fe1-N5	108.09(7)
		O5-Fe1-N5	100.99(7)
		N4-Fe1-N5	167.94(6)
(H_{2B}inaphydrazide)[Fe(2,6-pdc)$_2$			
Bond-length (Å)		Bond-angle (°)	
Fe1-O10	1.987(2)	O10-Fe1-O9	151.86(8)
Fe1-O9	2.005(18)	O10-Fe-1O4	94.17(9)
Fe1-O4	2.012(18)	O9-Fe-1O4	93.01(8)
Fe1-O7	2.047(18)	O10-Fe-1O7	93.36(8)
Fe1-N5	2.049(2)	O9-Fe1-O7	93.08(8)
Fe1-N4	2.051(2)	O4-Fe1-O7	151.70(8)
		O10-Fe1-N5	76.32(9)
		O9-Fe1-N5	75.97(8)
		O4-Fe1-N5	114.9(8)
		O7-Fe1-N5	93.38(8)
		O10-Fe1-N4	100.48(8)
		O9-Fe1-N4	107.65(8)
		O4-Fe1-N4	76.52(7)
		O7-Fe1-N4	75.29(7)
		N5-Fe1-N4	168.14(8)

Table S3: Selected examples of receptors used in the detection of Fe^{2+} and Fe^{3+} ions and detection limits.

Technique	Receptor	Comment	Detection limit	Reference
Colorimetric	Curcumin paper	Fe^{3+}	-	1S
	Silver nano-particle		25 μM	2S
	N-20-Hydroxyl-10-naphthyl methylene-3-hydroxyl-2-amino pyridine (NNAP)	Fe^{3+}	1.3 nM	3S
	6-Thiophen-2-yl-5,6-dihydrobenzo[4,5]imidazo-[1,2-c] quinazoline	Fe^{2+} and Fe^{3+}	3.7 nmol L^{-1} and 1.3 nmol L^{-1}	4S
	Superparamagnetic iron oxide nanoparticles, 1,10-phenanthroline	Fe^{2+} and Fe^{3+}	--	5S
	Complexometric 1,10-phenanthroline	Fe^{2+}	-	6S
	Fenton process	Fe^{2+}	-	7S
	1,10-phenanthroline	Fe^{2+} /Fe^{3+}	range of 1–10 μg ferrous iron	8S
	Ferrozine, 2,2′-bipyridine	Fe^{2+}	-	9S
	2,2′-Bipyridyl and with 2,2′,2′-terpyridyl.	Fe^{2+}	-	10S
	4,7-Diphenyl-1,10-phenanthroline	Fe^{2+}	-	11S
	1,10-Phenanthroline	Fe^{2+}	-	12S
	hydroxyl radicals	Fe^{2+}	-	13S
	Ag+ and 1,10-phenanthroline	Fe^{2+}	-	14S
Fluorescence	1,1-Bis(2-(((E)-(2-hydroxynaphthalene-1-yl)methylene)amino)ethyl)-3-(4-nitrophenyl)thiourea	Fe^{3+}	3.10 μM	15S
	Silver Nanoparticles/ biosurfactants	Fe^{2+} and Fe^{3+}	1 μM and 5 μM	16S
	quinoline derivative appended with rhodamine-6G	Selective over Fe2+	10^{-8} M	17S
	Carbon dots derived from cranberry beans	Fe^{3+}	9.55 μM	18S
	Cd-MOF of benzo-(1,2;3,4;5,6)-tris (thiophene-2'-carboxylic acid	Fe^{3+}	1.03 μM	19S
	Tetramethylpropylenediamine with phenylaceylene base conjugated oligomer-PPETE	Fe^{2+}/Fe^{3+}		20S
	SnS_2QDs	Fe^{3+}	0.84 μM	21S
	3-Amino-5-(thiazol-2-yl)-[1,1′-biaryl]-2,4-dicarbonitriles	Fe^{3+}	0.18 μM	22S
	Bi_2S_3-TiO_2 nanoparticles	Fe^{3+}	0.1173 μM	23S
	RhB–CdTe@SiO_2 QDs	Fe^{3+}	20.5 nM,	24S
	ATP C- nano dots		0.33μM	25S
	Zinc MOF of 2,5-bis(3′,5′-dicarboxylphenyl)-benzoic acid	Fe^{3+}	0.54ppm	26S
	B, N, S-*co*-doped carbon dots of 2,5-diaminobenzenesulfonic acid and 4-aminophenylboronic acid hydrochloride	Fe^{3+}	0.3–546 μM	27S
	La(III) MOF of 2,4,6-tri-p-carboxyphenyl pyridine	Fe^{3+}	16.6 μM	28S

	(Z)-2-(1-(3-Oxo-3H-benzo[f]chromen-2-yl)ethylidene)hydrazine-1-carbothioamid	Fe^{3+}	0.76 mM	29S
	Pyrene derivative	Fe^{3+}	-	30S
	3′,5,5′-Tetramethylbenzidine (TMB) dots (Near-infrared)	Fe^{3+}	0.17 μM	31S
	N-doped C-dots	Fe^{3+}	2.21 nM	32S
	Rhodamine-B armed fluorescent chemosensor		0.16 μm	33S
	N, N'-disubstituted imidazolium salts	Fe^{3+}	2.81×10^{-5} M	34S
	Amino acid-modified graphene quantum dots	Fe^{3+}	50nM	35S
	Biosurfactant capped silver nanoparticles	Fe^{2+} /Fe^{3+}	Distinguishes at μM level	36S
	Copper nanocluster	Fe^{3+}	10 nM	37S
	GQDs (Graphene quantum dots)	Fe^{3+}	-	38S
	GQDs with aspartic acid/ NH_4HCO_3	Fe^{3+}	260nM	39S
	GQDs with itric acid hydrazine	Fe^{3+}	90nM	40S
	GQDs with citric acid	Fe^{3+}	1000 nM	41S
	S-Doped GQDs	Fe^{3+}	4.2nM	42S
	Glyycine modified GQDs	Fe^{3+}	100nM	43S
	Rhodamine B modified GQDs,	Fe^{3+}	20nM	44S
	Polystyrenic anion-exchange resin with GQDs	Fe^{3+}	650 nM	45S
	MOF-derived c (ZIF-8C) GQDs	Fe^{3+}	80nM	46S
	Ordered C-SiO_2	Fe^{3+}	300nM	47S
	Nitrogen-GQDs	Fe^{3+}	0.22 μM,	48S
	Hydrazone modified GQDs	Fe^{3+}	2.5 μM	49S
	Amino-functionalized GQDs	Fe^{3+}	5.36 μM	50S
	GQDs with *Miscanthus* biorefinery waste	Fe^{3+}	1.41 nM	51S
	GQDs	Fe^{3+}	7220 nM	52S
	Rhodamine B hydrazide and naphthyl chromon turn on	Fe^{3+}	0.16 μM	53S
	Rhodamine–bistriazole	Fe^{3+}	0.15 μM	54S
	Functionalized Graphene Quantum Dots	Fe^{3+}	5.3 μM	55S
Voltametric	N-doped graphene quantum dots	Fe^{3+}	0.87 μM	56S
Colorimetric	Naphydrazide	Fe^{3+}	0.46 μM	This work
	2,6-H_2pdc	Fe^{3+}	1.28 μM	This work
	Naphydrazide and 2,6-H_2pdc	Fe^{3+}	0.09 μM	This work

Table S4: Selected examples of receptors used in detection of Cd^{2+} ions and detection limits.

Mode of sensing	Receptor	Detection limit	Reference	Comment
Visual	Bacterial whole-cell biosensor	0.034 μg/L	57S	-
Visual	Bacterial whole-cell Biosensor	26.7 nM	58S	
Conductance	Conducting bismuth encapsulated carbon nano-sheet	Sensitivity 0.48 μA μg^{-1}	59S	-
Conductance	Conducting polythiophene	-	60S	-

Fluorescence	Thiophene linked polypyridyl	-	61S	
Colorimetric	Semiconductin CdTe Q-dot	-	62S	-
Fluorescence	Squaramides	-	63S	Distinguishes Cd^{2+} /Zn^{2+}
Fluorescence	Thiophene-Appended Benzothiazole		64S	
Fluorescence	Vitamin B_6 Cofactor-Conjugate	59.0×10^8 M	65S	-
Aggregation induced emission (AIE)	Diimidazolylbenzene	-	66S	Turn-OFF Fe^{3+}
AIE	Cyclodextrin tetraphenylethene (TPE) and CD *via* click chemistry.	0.01 µM	67S	
AIE	*N*-(3-methoxy-2-hydroxybenzylidene)-3-hydroxy-2-naphthahydrazone	1.27×10^{-7} M	68S	Distinguishes Cd^{2+} /Zn^{2+}
NIR	Conjugated chain functionalized with amide of substituted amidoglycol	3.1 µM	69S	
Fluorescence	Rhodamine B + diethylenetetramine	1000 µg/L	70S	
Fluorescence	4-isobutoxy-6-(dimethylamino)-8-methoxyquinaldine	9.6 pM	71S	Distinguishes Cd^{2+} /Zn^{2+}
Colorimetric	Gold nano particles	5.35 pM	72S	
Fluorescence	(*S*,*S*)-*N*,*N*,*N*′,*N*′-tetrakis(6-methoxy-2-quinolylmethyl)-1,2-diphenylethylenediamine	-	73S	Cd^{2+} /Zn^{2+} interfere
Fluorescence	*N*,*N*,*N*′,*N*′-tetrakis(2-Quinolylmethyl)ethylenediamine	19 nM	74S	Zn^{2+} superior
Fluorescence	Di-2-Picolylamine-Substituted Quinoline-Based Tolans	158 nM	75S	
fluorescence	Perylene bisimide derivative with lactose and dipyridylamine	5.2×10^{-7} M	76S	
Fluorescence	4,4-Difluoro-4-bora-3a,4a-diaza-s-indacene (BODIPY derivative)	1.80×10^{-7} M	76S	Distinguishes Cd^{2+} /Zn^{2+}
Förster resonance energy transfer (FRET)	Quinoline–benzothiazole system	2.7×10^{-7} M	77S	-
Voltametric	Silver nanoparticles from Allium sativum	0.277 µM	78S	-
FRET	7-Amino-4-methylcoumarin	1.01×10^{-8} M)	79S	-
Fluorescence	2,2′-(Ethane-1,2-diylbis(oxy))bis(*N*,*N*-bis(pyridine-2-ylmethyl)aniline	3.77×10^4 M^{-1}	80S	Hg^{2+} interfere
Fluorescence	4,5-Quinolimide-based	11nM	81S	-
Fluorescence	2-6 Pyirdyl substituted Quinoline based	2.165×10^{-7} M	82S	No zinc interference
Fluorescence	Quinoline based receptor with cystine	Cd quench, Zn not	83S	-
Fluorescence	Carbazolone as fluorophore and *N*,*N*-bis(2-pyridylmethyl)ethylenediamine (BPEA) as chelator	-	84S	-
Fluorescence	Polyethylenimine-salicylaldehyde /Sulphide	10 nM	86S	Distinguish Cd^{2+} /Zn^{2+}
Voltametric	Anodic stripping voltammetry	1 ng/L	87S	-
	Carbon Dots	0.30 µM	88S	
Colorimetric	Peptide-modified gold nanoparticles	0.05 µM	89S	-
Fluorescence	Silver NPs	4.95 µM	90S	-
Fluorescence	L-Carnitine capped CdSe/ZnS quantum dots	0.15 µM	91S	-
Colorimetric	Chitosan dithiocarbamate functionalized gold nanoparticles	63 nM	92S	-
Fluorescence	Zn-Ag-In-S quantum dots	1.56 µM	93S	-
Fluorescence	Porphyrin-appended terpyridine	1.2×10^{-6} M	94S	-
Colorimetric	1-Amino-2-naphthol-4-sulfonic acid functionalized silver nanoparticles	87 nM	95S	-
Fluorescence	AuNPs with 4-amino-3-hydrazino-5-mercapto-1,2,4-triazole	30 nM	96S	-
Fluorescence	Fluorescein isothiocyanate QD	12 nM	97S	-
Colorimetric	Guanidine thiocyanate AuNPs	10 nM	98S	-
Fluorescence	Green-synthesized gold nanoparticles	1.13×10^{-10} M	99S	-

Fluorescence	L-Cysteine functionalized gold-silver nanoparticles	44 nM	100S	-
Fluorescence	Thioglycerolfunctionalized CdSe quantum dots	0.32 μM	101S	-
Colorimetric	Gold nanoparticle with 5-sulfosalicylic acid	3.0 nM	102S	-
Fluorescence	AgInZnS-QDs	37.8 nM	103S	-
Colorimetric	AuNPs with ssDNA	4.6 nM	104S	-
Fluorescence	AuNPs with di-(1H-pyrrol-2-yl) methanethione	16.6 nM	105S	-
Fluorescence	AuNPs Cysteamine and DL-glyceraldehyde	21 nM	106S	-
Fluorescence	NB-CQDs 2-amino-3-hydroxypyridine, sodium borohydride and L-cysteine	0.45 μM	107S	--
Fluorescence	Dialkyne and indole azide	2.69 μM	108S	-
Fluorescence	AuNPs 2,6-dimercaptopurine	3.66 μM	109S	-
Fluorescence	AgNPs Chalcon carboxylic acid	0.13 μM	110S	-
FRET	Spirolactam, xanthene and coumarin conjugate	1.01×10^{-8} M	111S	-
Fluorescence	{(H_2pip)[Mn(pydc-2,5)$_2$(H_2O)]·2H_2O}{H_2pip=piperazinediium, pydc-2,5=pyridine-2,5-dicarboxylate}	1.25 μM	112S	Zn^{2+} interfere
Fluorescence	Naphydrazide and 2,6-H_2pdc	18.31 μM	This work	

References for Table 3S and 4S:

1S. S. Wirojsaengthong, W. Aeungmaitrepirom, F. Unob, S. Fuangswasdi, P. Varanusupakul, K. Mueangdech, T. Treetos, P. Puthongkham, *J. Chem. Ed.,* 2023, **100**, 3604 – 3611.

2S. A. Ali, F. Hussain, S. Attacha, A. Kalsoom, W. A. Qureshi, M. Shakeel, J. Militky, B. Tomkova, D. Kremenakova, *Nanomaterials*, 2021, **11**, 2076.

3S. Z. Yan, Y. Zhu, J. Xu, C. Wang, Y. Zheng, P. Li, L. Hu and J. You, *Anal. Methods*, 2017, **9***,* 6240 – 6245.

4S. 3. S. Sen, S. Sarkar, B. Chattopadhyay, A. Moirangthem, A. Basu, K. Dhara, P. Chattopadhyay, *Analyst,* 2012, **137**, 3335 – 3342.

5S. C. Jiang, S. Yang, N. Gan, H. Pan, H. Liu, *J. Magn. Magn. Mater.*, 2017*,* **439**, 126 – 134.

6S. J. Zhu, X. Yang, F. Fan, Y. Li, *Appl, Water Sci.,* 2018, **8**, 228.

7S. L. Yang, G. Yao, *Int. J. Environ. Anal. Chem*. 2022, **102**, 3194 – 3206.

8S. 40. L. Herrera, P. Ruiz, J. C. Aguillon, A. Fehrmann, *J. Chem. Tech. Biotech*., 1989, **44**, 171 – 181.

9S. G. L. Smith, A. A. Reutovich, A. K. Srivastava, R. E. Reichard, C. H. Welsh, A. Melman, F. Bou-Abdallah, *J. Inorg. Biochem.*, 2021, **220** , 111460.

10S. M. L. Moss, M. G. Mellon, *Ind. Eng. Chem. Anal. Ed.,* 1942, **14**, 862 – 865.

11S. L. J. Clark, *Anal. Chem*., 1962, **34**, 348 – 352.

12S. H. Tamura, K. Goto, T. Yotsuyanagi, M. Nagayama, *Talanta,* 1974, **21**, 314 – 318.

13S. M. Tong, S. Yuan, S. Ma, M. Jin, D. Liu, D. Cheng, X. Liu, Y. Gan, Y. Wang, *Environ. Sci. Technol.,* 2016, **50**, 214 – 221.

14S. J. E. Amonette, J. Matyas, *Anal. Chim Acta*, 2016, **910**, 25 – 35.

15S. .S. Moon, M. Lee, C. Kim, *ChemistrySelect,* 2022, **7**, e202201353.

16S. K. Dayanidhi, N. Sheik Eusuff, *New J. Chem.,* 2021, **45**, 9936 – 9943.

17S. S. Das, K. Aich, S. Goswami, C. K. Quah, H. K. Fun, *New J. Chem.*, 2016, **40**, 6414 – 6420.

18S.M. Zulfajri, G. Gedda, C. -J. Chang, Y. P. Chang, G. Huang, *ACS Omega,* 2019, **4**, 15382 – 15392.

19S. P. Li, X. Chen, C. Guo, H. Zou, Z. Chen, B. Liu, W. Liang, J. Cai and H. Xu, *Eur. J. Inorg. Chem.*, 2023, **26**, e202200576

20S. M. E. A. Fegley, T. Sandgren, J. L. Duffy-Matzner, A. Chen, W. E. Jones Jr., *Polymer Chem.,* 2015, **53**, 951 – 954.

21S. R. R.Srivastava, V. K. Singh, A.Srivastava, *Optical Mater.,* 2020, **109**, 110337.

22S. B. Mariammal, A. Shylaja, S.V. Kumar, S. R. Rubina, R. R. Kumar, *J. Heterocyclic Chem*., 2020, **57**, 3882 – 3889.

23S. A. Syal, D. Sud, *Sensors and Actuators B: Chemical,* 2018, **266**, 1 - 8.

24S. H. Wu, L. Yang, L. Chen, F. Xiang, H. Gao, *Anal. Methods,* 2017, **9**, 5935 – 5942.

25S. J. Shangguan, J. Huang, D. He, X. He, K. Wang, R. Ye, X. Yang, T. Qing, J. Tang, *Anal. Chem.,* 2017, ***89***, 7477 – 7484.

26S. J. Wang, X. R. Wu, J. Q. Liu, B. H. Li, A. Singh, A. Kumar, S. R. Batten, *CrystEngComm*, 2017, **19**, 3519 – 3525.

27S. Y. Liu, W. Duan, W. Song, J. Liu, C. Ren, J. Wu, H. Chen, *ACS Appl. Mater. Interfaces,* 2017, **9**, 12663.

28S. J. Xia, Y. T. Zhuang, Y. L. Yu and J. H. Wang, *Microchim. Acta,* 2017, **184**, 1109 – 1116.

29S. G. M. Khairy, A,S. Amin, S, M. N. Moalla, A. Medhat, N. Hassan, *RSC Adv.*, 2022, *12*, 27679 – 27686.

30S. R.-X. Zhu, S. Yu, P. -B. Zhu, X. Gou, X. -Z. Yang, Hui Liu, L. -B. Xing, *J. Photochem. Photobio. A: Chemistry,* 2024, **450**, 115440.

31S. X. Qin, C. Chen, S. Zhang, J. Zhu, Y. Wang, J. Liu, *Anal. Methods*, 2019, **11**, 5007.

32S. P. Lesani, G. Singh, C. M. Viray, Y. Ramaswamy, D. M. Zhu, P. Kingshott, Z. Lu, H. Zreiqat, *ACS Appl. Mater. Interfaces*, 2020, **12**, 18395.

33S. D. Das, R. Alam, M. Sasmal, A. Katarkar, A. Dutta, M. Ali, *Inorg. Chim. Acta*, 2024, **563**, 121902.

34S. S. Chaudhary, M. D. Milton, *J. Photochem. Photobio. A: Chem.*, 2018, **356**, 595.

35S. Q. Ma, J. Song, S. Wang, J. Yang, Y. Guo, C. Dong, *Appl. Surf. Sci.,* 2016, **389**, 995 – 1002.

36S. H. Sharma, S. Chaudhary, S. Nirwan, R. Kakkar, H. S. Liew, M. L. Low, C. -W. Mai, L.-W. Hii, C. -O. Leong, M. D. Milton, *ChemistrySelect,* 2022, **7**, e202203239.

37S. H. Cao, Z. Chen, H. Zheng and Y. Huang, *Biosens. Bioelectron.,* 2014, **62**, 189 – 195.

38S. D. Wang, L. Wang, X. Dong, Z. Shi, J. Jin, *Carbon,* 2012, **50**, 2147 – 2154.

39S. C. F. Zhang, Y. Y. Cui, L. Song, X. F. Liu, Z. Hu, *Talanta,* 2016, **150**, 54 – 60.

40S. J. Ju, W. Chen, *Biosens. Bioelectron,* 2014, **58**, 219 – 225.

42S. T. Tran Van, T. Nguyen Bao, H. R. Kim, J. S. Chung, W. M. Choi, *Sens. Actuators B Chem.,* 2014, **202**, 568 – 573.

43S. S. H. Li, Y. C. Li, J. Cao, J. Zhu, L. Z. Fan, X. H. Li, *Anal. Chem.,* 2014, **86**, 10201 – 10207.

44S. L.B. Li, L. Li, C. Wang, K.Y. Liu, R.H. Zhu, H. Qiang, Y.Q. Lin, *Microchim. Acta*, 2015, **182**, 763 – 770.

45S. R. H. Guo, S. X. Zhou, Y. C. Li, X. H. Li, L. Z. Fan, N. H. Voelcker, *ACS Appl. Mater. Interfaces,* 2015, **7**, 23958 – 23966.

46S. A. Ananthanarayanan, X. W. Wang, P. Routh, B. Sana, S. Lim, D. H. Kim, K. H. Lim, J. Li, P. Chen, *Adv. Funct. Mater.,* 2014, **24**, 3021 – 3026

47S. W. J. Zhang, J. Gan, *Appl. Surf. Sci.,* 2016, **372**, 145 – 151.

48S. H. B. Xu, S. H. Zhou, L. L. Xiao, H. H. Wang, S.Z. Lia, Q. H. Yuan, *J. Mater. Chem. C,* 2015, **3**, 291 – 297.

49S. H. B. Xu, S. H. Zhou, L. L. Xiao, S. Z. Li, T. Song, Y. Wang, Q. H. Yuan, *Carbon*, 2015, **87**, 215 – 225.

50S. B. Zhang, Y. Luo, B. Peng, L. Zhang, N. Xie, D. Yue, W. Li, B. Qin, W. Du, Z. Wang, Y. Zhang, *J. Mol. Struct.*, 2024, **1304**, 137739.

51 S. -L. Ji, S. -S, Xiao,., L. -L. Wang, *Spectrochim. Acta A: Mol. Biomol. Spect.,* 2022, **280**, 121541.

52S. S. -F. Chin, S. -C. Tan, S.- C. Pang, S. -M. Ng, *Optical Materials*, 2017, **73**, 77 – 82.

53S. N. Vijay, S. P. Wu, S. Velmathi, *Journal of Photochemistry and Photobiology A: Chemistry*, 2019, **384**, 112060.

54S. K. Wechakorn, S. Chomngam, U. Eiamprasert, P. Kongsaeree, *Chem. Pap.*, 2021, **75**, 883.

55S. Kang, S., Han, H., Lee, K., Kim, K. M., *ACS Omega,* 2022, **7**, 2074 – 2081.

56S. Y. Fu, G. Gao, J. Zhi, *J. Mater. Chem. B*, 2019, **7**, 1494 – 1502.

57S. L. Shen, Y. Chen, L. Hu, C. Zhang, L. Liu, L. Bao, J. Ma, H. Wang, X. Xiao, L. Wu, S. Chen, *ACS Sensors,* 2024, **9**, 654 – 661.

58S. Z. Cui, X. Luan, H. Jiang, Q. Li, G. Xu, C. Sun, L. Zheng, Y. Song, P. A. Davison, W. E. Huang, *Chemosphere,* 2018, **200**, 322 – 329.

59S. Y. Feng, H. Zhao, T. Feng, X. Liu, M. Lan, *Microchemical J.,* 2024, **197**, 109881.

60S. Y. Sasaki, X. Lyu, T. Kawashima, Y. Zhang, K. Ohshiro, K. Okabe, K. Tsuchiya, T. Minami, *RSC Adv.*, 2024, **14**, 5159 – 5166

61S. E. Saravanan, M. Sathishkumar, J. Dhanapal, K., Selin, M, Iyer, S. Kulathu, *Anal. Chim. Acta* 2024, **1288**, 342179

62S. J. Cao, H. Jiang, Y. Wu, X. Yu, *Colloids and Surfaces B Bio-interfaces,* 2024, **235**, 113774.

63S. P. Lasitha, S. Dasgupta, P. G. Naresh, *ChemPhysChem,* 2020, **21**, 1564 – 1570.

64S. P. Purushothaman, S. Karpagam,. *ACS Omega,* 2022, **7**, 41361 – 41369,

65S. S. Bothra, P. Paira, A. Kumar, R. Kumar, S. K Sahoo, *ChemistrySelect*, 2017, **2**, 6023 – 6029

66S. C. Li, C. Gao, J. Lan, J. You, G. Gao, *Org. Biomol. Chem.*, 2014, **12**, 9524 – 9527.

67S. L. Zhang, W. Hu, L. Yu, Y. Wang, *Chem. Commun.*, 2015, **51**, 4298 – 5001.

68S. M. Wu, D. -D Yang, H. -W. Zheng, Q. -F. Liang, J. -B. Li, Y. Kang, S. Li, C. Jiao, X.-J. Zheng, L. -P. Jin, *Dalton Trans.*, 2021, **50**, 1507 – 1513.

69S. Y. Yang, T. Cheng, W. Zhu, Y. Xu, X. Qian, *Organic Letters* 2011, **13**, 264 – 267.

70S. Y. C. Reyes, T. B. Rouf, O. E. Torres, E. E. González, *ACS Agricultural Sci. Technol.,* 2022, **2**, 144 – 152.

71S. L. Xue, G. Li, Q. Liu, H. Wang, C. Liu, X. Ding, S. He, H. Jiang, *Inorg. Chem*., 2011, **50**, 3680 – 3690.

72S. M. Bhattacharyya, M. Hossain, *J. Environ. Chem. Eng.*, 2024, **2** , 112295.

73S. Y. Mikata, K. Nozaki, M. Tanaka, H. Konno, A. Matsumoto, M. Kawamura, S. -I. Sato, *Inorg. Chem.*, 2020, **59***,* 5313 – 5324.

74S. Y. Mikata, M. Kaneda, S. Yonemura, M. Akedo, H. Konno, T. Matsuo, *Dalton Trans.,* 2022, **51**, 17170 – 17179.

75S. M. -S. Ko, P. S. Rao, D. -G. Cho, *Molecules,* 2021, **26***,* 917.

76S. J. -K, Xiong, K, -R. Wang, K. -X. Wang, T. -L. Han, H.-Y. Zhu, R.-X. Rong, Z. -R. Cao, X.-L. Li, *Sensors and Actuators B: Chem.*, 2019, **297**, 126802.

77S. A. Maity, U. Ghosh, D. Giri, D. Mukherjee, T. K. Maiti, S. K. Patra, *Dalton Trans.,* 2019, **48**, 2108 – 2117.

78S. K. Aich, S. Goswami, S. Das, C. D. Mukhopadhyay, C. K. Quah, H.-K. Fun, *Inorg. Chem.,* 2015, **54**, 7309 – 7315.

79S. A. Aravind, M. Sebastian, B. Mathew, *New J. Chem.,* 2018, **42**, 15022 – 15031.

80S. S. B. Maity, S. Banerjee, K. Sunwoo, J. S. Kim, P. K. Bharadwaj, *Inorg. Chem*., 2015, **54**, 3929 – 3936.

81S. Y. Zhang, X. Guo, M. Zheng, R. Yang, H. Yang, L. Jia, M. Yang, *Org. Biomol. Chem.,* 2017, **15**, 2211 – 2216.

82S. Z. Xu, G. Li, Y.-Y. Ren, H. Huang, X. Wen, Q. Xu, X. Fan, Z. Huang, J. Huang, L. Xu. *Dalton Trans.,* 2016, **45**, 12087 – 12093.

83S. Y. Ma, F. Wang, S. Kambam, X. Chen, *Sensors and Actuators B: Chem.,* 2013, **188,** 1116 – 1122.

84S. Q. -C. Xu, X. -H. Zhu, C. Jin, G. -W. Xing, Y. Zhang, *RSC Adv*., 2014, **4**, 3591 – 3596.

85S. X. -Y. Liu, D. -Y. Liu, J. Qi, Z. -G. Cui, H. -X. Chang, H. -R. He, G. -M. Yang, *Tett. Letters* 2015, **56**, 1322 – 1327.

86S. N. -D. Tan, J. -H. Yin, G. Pu, Y. Yuan, L. Meng, N. Xu, *Chem. Phys. Lett.*2016, **666**, 68 – 72.

87S. L. Mart, H. W. Nuernberg, P. Valenta, *Zeitschrift fuer Analytische Chemie,* 1980, **300**, 350 – 362.

88S. Y. Xu, C. Wang, T. Jiang, G. Ran, Q. Song, *J. Hazard. Mater.,* 2022, **427**, 128092

89S. M. Zhang, Y. Q. Liu, B. C. Ye, *Analyst*, 2012, **137**, 601 – 607.

90S. S. Jabariyan, M. A. Zanjanchi, *Appl. Phys. A*, 2019, **125**, 872.

91S. H. B. Li, Y. Zhang, X. Q. Wang, *Sensors and Actuators B Chem.,* 2007, **127,** 593 – 597.

92S. V. N. Mehta, H. Basu, R. K. Singhal, S. K. Kailasa,. *Sensors and Actuators B: Chem.,* 2015, **220**, 850 – 858.

93S. C. Wei, X. Wei, Z. Hu, D. Yang, S. Mei, G. Zhang, D. Su, W. Zhang, R. Guo, *Anal. Methods,* 2019, **11**, 2559 – 2564.

94S. H. -Y. Luo, J. -H. Jiang, X. -B. Zhang, C. -Y. Li, G. -L. Shen, R. -Q. Yu, *Talanta*, 2007, **72,** 575 – 581.

95S. P. Huang, B. Liu, W. Jin, F. Wu, Y. Wan, *J. Nanopart. Res*., 2016, **18,** 327.

96S. A. -J. Wang, H. Guo, M. Zhang, D. -L. Zhou, R. -Z. Wang, J. -J. Feng, *Microchim. Acta*, 2013, **180,** 1051 – 1057.

97S. R. Gui, X. An, W. Huang, *Anal. Chim. Acta*, 2013, **767,** 134 – 140.

98S. J. R. Bhamore, A. R. Gul, S. K. Kailasa, K. -W. Kim, J. S. Lee, H. Park, T. J. Park, *Sensors and Actuators B Chem.,* 2021, **334,** 129685.

99S. K. Singh, V. Kumar, B. Kukkar, K. H. Kim, T. R. Sharma, *J. Envron. Sci. Technol*., 2022, **19**, 4673 – 4690.

100S. J. Du, X. Hu, G. Zhang, X. Wu, D. Gong, *Anal. Lett.,* 2018, **51**, 2906 – 2919.

101S. N. B. Brahim, N. B. H. Mohamed, M. Echabaane, M. Haouari, R. B. Chaabane, M. Negrerie, H. B. Ouada, *Sensors and Actuators B Chem.,* 2015, **220**, 1346 – 1353.

102S. W. Jin, P. Huang, F. Wu, L. -H. Ma, *Anal*yst, 2015, **140**, 3507 – 3513.

103S. Y. Liu, X. Tang, M. Deng, T. Zhu, L. Edman, J. Wang, J. *Alloy. Compd.,* 2021, **864**, 158109.

104S. Y. Wu, S. Zhan, L. Wang, P. Zhou, *Analyst*, 2014, *139*, 1550 – 1561.

105S. Y. -M. Sung, S. -P. Wu, *Sensors and Actuators B Chem*., 2014, **201**, 86 – 91.

106S. R. Yadav, P. N. Patel, V.N. Lad, *Res. Chem. Intermed.*, 2018, **44**, 1 – 13.

107S. Z. Yan, W. Yao, K. Mai, J. Huang, Y. Wan, L. Huang, B. Cai, Y. Liu, *RSC Adv*., 2022, **12**, 8202 – 8210.

108S. Y. Tang, H. Liu, G. Jiang, Z. Gu, *J. Appl. Spectrosc*., 2017, **84,** 911 – 914.

109S. M.H. Hu, W.H. Huang, L.L. Suo, L.H. Zhou, L.F. Ma, H. F. Zhu, *Anal. Methods*, 2017, **9,** 5598 – 5603.

110S. Y. Dong, L. Ding, X. Jin, N. Zhu, *Microchim. Acta*, 2017, **184**, 3357 – 3362.

111S. C. Kumari, D. Sain, A. Kumar, S. Debnath, P. Saha, S. Dey. *Dalton Trans*., 2017, **46**, 2524 – 2531

112S. K. K. Singha, P. Majee, S. K. Mondal, P. Mahata, *ChemistrySelect,* 2017, **2**, 3388 – 3395.

113S. M. Zhu, C. Shi, X. Xu, Z. Guo, W. Zhu, *RSC Adv*., 2016, **6**, 100759 – 100764.

Table S5: Standard deviations in the detection of cadmium ions by fluorescence at 400 nm of a solution of Naphydrazide (2 mM, 2.5 mL) together with 2,6-H_2pdc (20 mM, 400 μL) after incremental addition of 20 mM Cd^{2+} in two independent experiments

(a)

Volume of Cd^{2+} added (μL)	Reading of Fluorescence Emission Intensity after three minutes (count per sec)			Mean	Standard Deviation (σ)
0	5423.213	5152.456	5590.167	5388.612	220.897
50	43631.000	44851.740	44291.810	44258.180	611.063
100	95905.350	95518.450	93187.510	95537.103	359.283
150	133052.100	133687.500	133988.700	133576.100	478.134
200	186589.600	187349.400	187507.300	187148.800	490.615
250	258397.100	257512.500	258264.800	258058.100	477.14
300	341005.200	341802.900	341110.400	341306.200	433.384

(b)

Volume of Cd^{2+} added (μL)	Reading of Fluorescence Emission Intensity after three minutes (count per sec)			Mean	Standard Deviation (σ)
0	5574.425	5080.312	5270.3250	5308.367	249.238
50	48351.480	48890.650	47905.540	48382.560	493.28
100	93870.210	93252.710	94087.670	93736.860	433.157
150	120568.205	120930.480	121510.820	121003.168	475.492
200	186041.709	185256.910	185340.540	185546.400	430.995
250	265139.693	265354.512	264473.109	264989.105	459.592
300	353364.795	354162.629	353290.106	353726.367	483.634